Repeated exposure of human skin fibroblasts to UVB at subcytotoxic level triggers premature senescence through the TGF-β1 signaling pathway

Florence Debacq-Chainiaux[1], Céline Borlon[1], Thierry Pascal[1], Véronique Royer[1], François Eliaers[1], Noëlle Ninane[1], Géraldine Carrard[2], Bertrand Friguet[2], Françoise de Longueville[3], Sophie Boffe[3], José Remacle[1] and Olivier Toussaint[1,*]

[1]Laboratory of Biochemistry and Cellular Biology, Department of Biology, University of Namur (FUNDP), Rue de Bruxelles, 61, 5000 Namur, Belgium
[2]Laboratoire de Biologie et Biochimie Cellulaire du Vieillissement – EA 3106 – Université Paris 7, France
[3]Eppendorf Array Technologies, Rue du Séminaire, 12, 5000 Namur, Belgium
*Author for correspondence (e-mail: olivier.toussaint@fundp.ac.be)

Accepted 17 November 2004
Journal of Cell Science 118, 743-758 Published by The Company of Biologists 2005
doi:10.1242/jcs.01651

Summary

Premature senescence of human diploid fibroblasts (HDFs) can be induced by exposures to a variety of oxidative stress and DNA damaging agents. In this study we developed a robust model of UVB-induced premature senescence of skin HDFs. After a series of 10 subcytotoxic (non-proapoptotic) exposures to UVB at 250 mJ/cm^2, the so-called biomarkers of senescence were markedly expressed: growth arrest, senescence-associated β-galactosidase activity, senescence-associated gene overexpression, deletion in mitochondrial DNA. A set of 44 stress- and senescence-associated genes were found to be differentially expressed in this model, among which clusterin/apolipoprotein J (apo J) and transforming growth factor-β1 (TGF-β1). Transfection of apo J cDNA provided protection against premature senescence-inducing doses of UVB and other stressful agents. Neutralizing antibodies against TGF-β1 or its receptor II (TβRII) sharply attenuated the senescence-associated features, suggesting a role for TGF-β1 in UVB-induced premature senescence. Both the latent and active forms of TGF-β1 were increased with time after the last UVB stress. Proteasome inhibition was ruled out as a potential mechanism of UVB-induced stress-induced premature senescence (SIPS). This model represents an alternative in vitro model in photoaging research for screening potential anti-photoaging compounds.

Supplementary material available online at
http://jcs.biologists.org/cgi/content/full/118/4/743/DC1

Key words: Fibroblasts, senescence, UVB, clusterin, transforming growth factor beta-1, proteasome, protein oxidation

Introduction

The definition of replicative senescence covers irreversible growth arrest triggered by telomere shortening which counts generations of cells lacking endogenous telomerase (Shay and Wright, 2000). Cells can remain alive for several months after the onset of replicative senescence (Bayreuther et al., 1988). In contrast, cells committed to apoptosis die with hours after pro-apoptotic stimuli (Zhivotovsky and Kroemer, 2004).

Exposure of human proliferative cell types such as human diploid fibroblasts (HDFs), endothelial cells, melanocytes, etc. to acute stress from subcytotoxic concentrations of oxidative agents such as *tert*-butylhydroperoxide (*t*-BHP) (Dumont et al., 2000) or hydrogen peroxide (H_2O_2) (Chen et al., 1998), results in stress-induced premature senescence (SIPS) which begins 2-3 days after the stress (Brack et al., 2000), long before the cells reach the critical telomere length observed in replicative senescence. Cells in SIPS induced by subcytotoxic oxidative stress remain alive for months (Dumont et al., 2000; Bayreuther et al., 1988) and display several features of replicative senescence. These features include a typical senescent morphology (Bayreuther et al., 1988), senescence-associated β-galactosidase (SA β-gal) activity (Dimri et al., 1995), deletion in mitochondrial DNA (Dumont et al., 2000) and change in the expression level of several senescence-associated genes such as *clusterin/apolipoprotein J* (*apo J*), coding a protein with extracellular chaperone-like activity (Dumont et al., 2000). Transforming growth factor-β1 (TGF-β1) signaling pathway also regulates the appearance of the features of H_2O_2-induced premature senescence (Frippiat et al., 2001). In addition cells in SIPS display long-term stress-specific irreversible mRNA and protein expression level changes coined 'molecular scars' (Dierick et al., 2002).

UVB (290-320 nm) is an inherent component of sunlight that crosses the epidermis, reaching the upper dermis composed mainly of fibroblasts and extracellular matrix (Rosette and Karin, 1996). UVB interacts with cellular chromatophores and photosensitizers resulting in the generation of reactive oxygen species (ROS), DNA damage and activation of signaling pathways related to growth, differentiation, senescence and connective tissue degradation (Helenius et al., 1999). Preliminary data demonstrated the feasibility of detecting biomarkers of senescence in skin HDFs

after subcytotoxic exposures to UVB. Unfortunately only a low number of stresses was performed, which did not produce highly expressed biomarkers of senescence or permit mechanistic studies (Chainiaux et al., 2002).

In this work, we present a new model of SIPS obtained by exposing skin HDFs to a series of 10 non-pro-apoptotic stresses with subcytotoxic doses of UVB. This treatment induced marked appearance of senescence-associated features and changes in gene expression profiles. It was therefore possible to study the potential role of two systems known as being protective against the appearance of modified proteins: apo J and the proteasome. Indeed we could test if ectopic overexpression of apo J protects against UVB-induced cytotoxicity and premature senescence and measured both the proteasome activity and level of oxidized proteins when SIPS establishes. We were also able to test the involvement of TGF-β1 in UVB-induced SIPS.

Materials and Methods

Cell culture, exposure to UVB, cytotoxicity assay and SA β-galactosidase activity

AG04431 skin HDFs (Coriell Institute for Medical Research, USA) were classically grown in BME (basal medium Eagle) (Invitrogen, UK) + 10% (v:v) fetal calf serum (FCS) (Invitrogen, UK) and 2 mM L-glutamine and 100 μg/ml streptomycin. Cells at 55-60% of in vitro proliferative life span were subcultured at half confluence (10,000 cells/cm^2) in BME + 1% FCS. At 72 hours after plating, they were washed once with phosphate-buffered saline pH 7.4 (10 mM, 0.9 g NaCl) (PBS) and exposed to UVB radiation in a thin layer of PBS using three Philips TL 20W/01 lamps (Philips, The Netherlands), emitting UVB peaking at 311 nm, which were placed 30 cm above the flasks. The emitted radiation was checked under the flask lid using a UVR radiometer with a UVB sensor (Bioblock Scientific, Belgium). After irradiation, PBS was replaced by BME + 1% FCS. The radiation stress was performed twice a day for 5 days. Control cells were kept in the same culture conditions without UVB exposure.

At 48 hours after the last stress, the cellular protein content was assayed by the Folin method described by Lowry (Lowry et al., 1951). This method was previously shown to give accurate estimates of the number of surviving cells in such conditions (Dumont et al., 2000). The results (mean of triplicates ± s.d.) are expressed as a percentage of surviving cells. Alternatively, cells were seeded 48 hours after the last stress in square 35 mm culture dishes (Falcon, UK) at 700 cells/cm^2 in BME + 1% FCS. Senescence-associated β-galactosidase (SA β-gal) activity was determined 24 hours later as described by Dimri et al. (Dimri et al., 1995). The population of SA β-gal-positive cells was determined by counting 400 cells per dish. The proportions of cells positive for the SA β-gal activity are given as percentage of the total number of cells counted in each dish. The results are expressed as mean of triplicates ± s.d.

SV-40 transformed WI-38 fibroblasts (#CCL-75.1, WI-38 VA-13 subline 2RA) purchased from the American Type Culture Collection (USA) were seeded at 200,000 cells/well of 10 cm^2 multidishes (Cel Cult, UK). At 24 hours after seeding, the cells were exposed to a single 1-hour stress under increasing concentrations of *tert*-butylhydroperoxide (*t*-BHP) (0-500 μM) (Merck, Germany), a 2-hour stress under ethanol (0-10%) diluted in minimal essential medium (MEM; Invitrogen, UK), or a UVB stress performed (0-4500 mJ/cm^2) in a thin layer of PBS. After rinsing twice with MEM, the cells were given fresh MEM + 10% FCS. Cell survival was assessed 24 hours after the stress using the classical method of cellular protein assay (Lowry et al., 1951).

Estimation of DNA synthesis and protein level of p53, p21^{WAF-1} and p16^{INK-4a}

At 24, 48 and 72 hours after the last stress, cells were seeded in 24-well plates (Cell Cult, UK) at 10,000 cells/well in BME + 1% FCS. 1 μCi [^{3}H]thymidine (specific activity: 2 Ci/mmol; Du Pont, NEN, USA) was added to BME + 1% FCS for 48 hours. Quantification of radioactivity was performed using a scintillation counter (Packard Instrument Company, USA) as described by Dumont et al. (Dumont et al., 2000). The results are expressed as mean of triplicates ± s.d.

At 72 hours after the last stress, cells were washed once with PBS and lysed on ice [2% SDS, 10 mM Tris, 1 mM EDTA pH 6.8, anti-protease complete (Roche, Germany)]. After homogenization of the lysates, 30 μg of proteins were electrophoresed on Bis-Tris NuPage 4-12% acrylamide gel (Invitrogen, UK). The proteins were transferred on hybond-P membrane (Amersham Biosciences, Sweden). The antibodies used were anti-p53 antibody (sc-6243), anti-p21^{WAF-1} antibody (sc-6246), anti-p16^{INK-4} antibody (sc-468) (Santa Cruz Biotechnology, USA), anti-α-tubulin antibody (AM2495-11, Innogenex, USA) and horseradish peroxidase-linked secondary antibody (Amersham Biosciences, Sweden). The bands were visualized chemiluminescently (ECL Advance Detection Kit, Amersham Biosciences, Sweden). Semi-quantification was obtained with ImageMaster TotalLab software (Pharmacia, Sweden).

Real time RT-PCR

At 72 hours after the last stress, total RNA was extracted from three independent cultures using the Total RNAgent extraction kit (Promega, USA). Total RNA (2 μg) was reverse transcribed using SuperScript II Reverse Transcriptase (Invitrogen, UK). Primers (Table 1A) were designed using the Primer Express 1.5 software (Applied Biosystems, The Netherlands). Amplification reactions assays contained 1× SYBR Green PCR Mastermix and primers (Applied Biosystems, The Netherlands) at optimal concentration. A hot start at 95°C for 5 minutes was followed by 40 cycles at 95°C for 15 seconds and 65°C for 1 minute using the 7000 SDS thermal cycler (Applied Biosystems, The Netherlands). Melting curves were generated after amplification and data were analyzed using the thermal cycler software. Each sample was tested in triplicate.

Low density DNA-array

Design of the array

We developed the DualChip™ human aging, a low-density DNA array representing a range of 240 genes involved in senescence or stress response of HDFs in collaboration with Eppendorf (Germany) (see Table S1 in supplementary material). The method is based on a system with two assays (a control and a test) per glass side with three sub-arrays per assay. The sequences of the DNA covalently linked to the glass slide were carefully chosen by sequence comparison. Checks were made to ensure that no cross-hybridization takes place. Several positive and negative hybridization controls plus detection controls were spotted on the array in order to control the reliability of the experimental data. 0.5 μg of mRNA was retrotranscribed using SuperScript II Reverse Transcriptase (Invitrogen, UK). Three synthetic poly(A)$^+$ tailed RNA standards were spiked at three different amounts (10 ng, 1 ng and 0.1 ng per reaction) into the purified mRNA. Three independent experiments were performed in triplicate, providing hybridizations on nine arrays. Hybridization on DualChip human aging was carried out as described by the manufacturer. Detection was performed using a Cy3-conjugated IgG anti-biotin (Jackson Immuno Research Laboratories, USA). Fluorescence of the hybridized arrays was scanned using the Packard ScanArray (PerkinElmer, USA) at a resolution of 10 μm. To maximize the dynamic range of detection, the same arrays were scanned at three photomultiplier gains for quantifying high- and low-copy expressed genes. The scanned 16-bit images were imported into the ImaGene

Table 1. Primers

A. Real time PCR primers

Genes	Positions (bp)	Sequences
Apolipoprotein J	937-959	5′-gga tga agg acc agt gtg aca ag-3′
	1032-1050	5′-cag cga cct gga ggg att c-3′
Fibronectin	5023-5041	5′-tgt ggt tgc ctt gca cga t-3′
	5111-5131	5′-gct tgt ggg tgt gac ctg agt-3′
Osteonectin	868-889	5′-gag acc tgt gac ctg gac aat g-3′
	957-982	5′-gga agg agt gga ttt aga tca caa ga-3′
SM22	511-530	5′-cgt gga gat ccc aac tgg tt-3′
	586-606	5′-aag gcc aat gac atg ctt tcc-3′
p21WAF-1	495-515	5′-ctg gag act ctc agg gtc gaa-3′
	599-617	5′-cca gga ctg cag gct tcc t-3′
p53	1209-1229	5′-aag aaacca ctg gat gga gaa-3′
	1263-1283	5′-cag ctc tcg gaa cat ctc gaa-3′
c-fos	249-268	5′-tca ccc gca gac tcc ttc tc-3′
	323-343	5′-gtg gga atg aag ttg gca ctg-3′
c-jun	2016-2033	5′-gga tca agg cgg aga gga a-3′
	2088-2102	5′-tcc agc cgg gcg att-3′
TGF-β1	1788-1808	5′-agg gct acc atg cca act tct-3′
	1869-1889	5′-ccg ggt tat gct ggt tgt aca-3′
TGF-β2	1067-1083	5′-acc aac cgg cgg aag aa-3′
	1153-1176	5′-cac cct aga tcc ctc ttg aaa tca-3′
TGF-β3	1288-1305	5′-agg ccc ttg ccc ata cct-3′
	1349-1372	5′-aga tgc ttc agg gtt cag agt gtt-3′
GAPDH	942-963	5′-acc cac tcc tcc acc ttt gac-3′
	1033-1053	5′-gtc cac cac cct gtt gct gta-3′

B. Primers used for the detection of the common 4977 bp mitochondrial DNA deletion

Primers	Positions (bp)	Sequences
H1	219-238	5′-atg ctt gta gga cat aat aa-3′
L1	447-466	5′-agt ggg agg gga aaa taa ta-3′
H2	8150-8169	5′-ccg ggg gta tac tac ggt ca-3′
L2	13631-13650	5′-ggg gaa gcg agg ttg acc tg-3′
H3	8197-8215	5′-cag ttt cat gcc cat cgt c-3′
L3	13560-13578	5′-gat gag agt aat aga tag g-3′

C. Primers used to construct the different apo J retroviral expression vectors

Primers	Sequences
APOJ31F	5′-cgc gga tcc gcg gcg acc atg atg aag act ctg ctg ctg tt-3′
APOJ31R	5′-tgc tct aga gcc ctc ctc ccg gtg ctt ttt gcg-3′
APOJPNF	5′-g ggt taa ccc gcc acc atg atg aag act ctg ctg ctg tt-3′
APOJPNR	5′-c ggg atc ccg gcg ggt tta aac tca atg gtg-3′
TRAPOJR	5′-c ggg atc ccg tca ctc ctc ccg gtg ctt ttt gc-3′

4.1 software (BioDiscovery, USA). The fluorescence intensity of each DNA spot (average intensity of each pixel present within the spot) was calculated using local mean background subtraction. A signal was accepted when the average intensity after background subtraction was at least 2.5-fold higher than their local background. The three intensity values of the triplicate DNA spots were averaged and used to calculate the intensity ratio between the reference and the test samples.

Data normalization

The data were normalized in two steps. First, the values were corrected using a factor calculated from the intensity ratios of the internal standards in the references and test samples. The presence of the three internal standard probes at two different locations of the array allowed a measurement of local background and evaluation of the array homogeneity, which is considered in the normalization. However, since the internal standard control does not take into account the purity and quality of the mRNA, a second step of normalization was performed based on calculating the average intensity for a set of eight housekeeping genes. The variance of the normalized set of housekeeping genes was used to generate an estimate of expected variance, leading to a predicted confidence interval for testing the significance of the ratios obtained. Ratios outside the 95% confidence interval were determined to be significantly different (de Longueville et al., 2002; de Magalhaes et al., 2004).

Detection of the common 4,977 bp mitochondrial DNA deletion

Mitochondrial DNA was extracted as described previously (Filser et al., 1997) and the presence of mitochondrial DNA was assessed by PCR amplification of a 247 bp conservative region of the mitochondrial DNA using H1/L1 as described by Berneburg et al. (Berneburg et al., 1999). Nested PCR, to detect the deletion, was performed with H2/L2 and H3/L3 primers as described previously (Dumont et al., 2000). Sequences of the primers are shown in Table 1B. PCR was carried out with 500 ng of mitochondrial DNA, 2.5 U AmpliTaq Gold Polymerase (Roche, Germany), 200 μM dNTPs and 1 μM of the primers. After initial denaturation (94°C, 10 minutes), PCR conditions, according to the respective primers were: [H1/L1] denaturation, 94°C, 1 minute; annealing, 58°C, 1 minute; elongation, 72°C, 45 seconds; 30 cycles; [H2/L2] denaturation, 94°C, 30 seconds; annealing, 55°C, 35 seconds; elongation, 72°C, 1 minute; 40 cycles; [H3/L3] denaturation, 94°C, 30 seconds; annealing, 52°C, 45 seconds; elongation, 72°C, 1 minute; 25 cycles. Final elongation (72°C, 10 minutes) was the last step of all these PCRs. PCR products were detected with ethidium bromide after agarose gel electrophoresis. The first set of primers (H2/L2) flanking the deletion gives a 524 bp fragment and the set of nested primers (H3/L3) give a 404 bp fragment. Nested PCR was carried out with 1 μl of the 50 μl mixture obtained with the H3/L3 primers.

Anti-active caspase-3 immunofluorescence

Cells were seeded at 1,000 cells/cm^2 in BME +1% FCS on glass cover slides at 72 hours before incubation with TGF-β1. Alternatively, cells were seeded at 1,000 cells/cm^2 in BME +1% FCS at 16, 40 or 64 hours after the last UVB stress. As a positive control of pro-apoptotic stimuli, cells were incubated for 16 hours in BME + 25 μM etoposide (Sigma, USA). After incubation, the cells were fixed for 10 minutes with 4% paraformaldehyde (Merck, Germany) in PBS before three washings with PBS. Cells were permeabilized in PBS + 1% Triton X-100 (Sigma, USA) and then washed twice in PBS + 3% bovine serum albumin (BSA) (Sigma, USA). The specific rabbit polyclonal antibody against anti-active caspase-3 (1:100 dilution, Promega, USA) was added overnight at 4°C in a wet room. The cells were washed three times in PBS + 3% BSA before adding the specific Alexa Fluor 488 goat anti-rabbit IgG (H+L) conjugate (1:1000 dilution; Molecular Probes, USA) diluted in PBS + 3% BSA for 1 hour in a wet room at room temperature. The cells were washed three times in PBS + 3% BSA. To visualize the nucleus, the cells were incubated for 35 minutes at room temperature with TO-PRO-3 [1:80 dilution (Molecular Probes, USA) in PBS + 2 mg/ml RNAse (ICN, USA)]. The coverslips were mounted in Mowiol (Sigma, USA) and observed with a TCS confocal microscope (Leica, Germany) using a constant multiplier.

PARP cleavage

After the TGF-β1 stimulation and at 4, 16, 40 or 64 h after the last UVB-stress, the cells were washed once with PBS and lysed on ice (2% SDS, 10 mM Tris, 1 mM EDTA pH 6.8, anti-protease complete; Roche, Germany). As positive control of pro-apoptotic stimuli, cells were exposed to *t*-BHP at cytotoxic concentrations. After homogenization of the lysates, 30 μg of proteins were subjected to SDS-PAGE (10% acrylamide) and transferred to a PVDF membrane (Amersham Biosciences, Sweden). The antibodies were a specific mouse monoclonal anti-PARP antibody (#556494, BD Biosciences, USA), anti-α-tubulin antibody (AM2495-11, Innogenex, USA) and

horseradish peroxidase-linked secondary antibody (Amersham Biosciences, Sweden). The bands were visualized chemiluminescently (ECL Advance Detection Kit; Amersham Biosciences, Sweden). Semi-quantification was obtained with the ImageMaster TotalLab software (Pharmacia, Sweden).

Transfection of apolipoprotein J cDNA

Cloning of *apo J* cDNA

A 1350 bp complementary deoxyribonucleic acid (cDNA) fragment containing the entire open reading frame of human *apo J* (RZPD, Germany) was amplified by PCR from the pBluescript II SK plasmid using forward primer APOJPNF (Table 1C) (*Hpa*I restriction site at 5′ end) and TRAPOFR (*Bam*HI restriction site at 5′ end). The purified amplicons were digested by *Hpa*I and *Bam*HI and inserted using a T4 ligase reaction (Promega, USA) into the pLXSN retroviral vector (Clontech, USA).

Cloning of *apo J* V5/His tag cDNA

The 1350 bp cDNA fragment of human *apo J* was amplified by PCR from the pBluescript II SK plasmid using forward primer APOJ31F (*Bam*HI restriction site at 5′ end) and reverse primer APOJ31R (*Xba*I restriction site at 5′ end). The purified amplicons were digested by *Bam*HI and *Xba*I and inserted using a T4 ligase reaction into the pCDNA3.1 V5/His (Clontech, USA). The apo J V5/His sequence was amplified by PCR using forward primer APOPNF (*Hpa*I restriction site at 5′ end) and reverse primer APOPNR (*Bam*HI restriction site at 5′ end). The purified amplicons were digested by *Hpa*I and *Bam*HI and inserted using a T4 ligase reaction into the pLXSN retroviral vector. The different constructs were checked by restriction profiles and sequencing (data not shown).

Transfections

Subconfluent SV-40 WI-38 cells (# CCL-75.1, American Type Culture Collection, USA) were cultured in 100 mm culture dishes (Cel Cult, USA) containing 10 ml of MEM (Invitrogen, USA) without serum and were transfected for 8 hours with 30 μg of either pLXSN/apo J expression vector, pLXSN/apo J-V5-His expression vector or pLXSN vector without insert, using $Ca_2(PO_4)_3$ precipitation method (CalPhos mammalian transfection kit; Clontech, USA). At 48 hours after transfection, the cells were plated and exposed to the selection medium containing 0.5 mg/ml G418 (Invitrogen, USA). Colonies were isolated after 3 weeks of selection and expanded in MEM + 10% FCS supplemented with 0.5 mg/ml G418.

Overexpression of apo J in AG04431 HDFs between 35 and 40% of the replicative lifespan was achieved by retroviral infections. The pLXSN/apo J expression vector, the pLXSN/apo J-V5-His expression vector and the pLXSN vector without insert were transfected in the PT67-packaging cell line (Invitrogen, USA) by $Ca_2(PO_4)_3$ precipitation. After 15 days of selection under 0.5 mg/ml G418, stable virus-producing cell lines were obtained. At 18 hours prior the infections, AG04431 HDFs were plated in 100 mm culture dishes at 500,000 cells/dish. The culture medium of PT67 cells accumulated viruses for 3 days. This medium was collected, filtered through a 0.45 μm filter (Sarstedt, Germany) and supplemented with 4 μg/ml of hexadimethrine bromide (Sigma, USA). The retroviral supernatants were added (10 ml/dish) to the target AG04431 cells for 24 hours. At day 2 after the infection, a 2-week selection under 0.5 mg/ml G418 was started.

To check for apo J overexpression at the protein level, cell lysates were prepared in lysis buffer (2% SDS, 10 mM Tris, 1 mM EDTA pH 6.8, anti-protease complete; Roche, Germany). We used anti-clusterin β (Santa Cruz, USA) and anti-V5 (Invitrogen, UK) antibodies. The level of α-tubulin was used as reference level.

Proteasome peptidase activities

Proteasome activities were monitored using fluorogenic peptides, LLVY-AMC (Succinyl-Leu-Leu-Val-Tyr-7-amido-4-methylcoumarin) for the chymotrypsin-like and LLE-NA (N-benzyloxycarbonyl-Leu-Leu-Glu-β-naphthylamine) for the peptidylglutamyl-peptide hydrolase activities, as previously described (Bulteau et al., 2000). The assay mixture contained 50 μg of total soluble protein in 25 mM Tris-HCl buffer, pH 7.5 and the fluorogenic peptide was added at different concentrations (25 μM for LLVY-AMC and 150 μM for LLE-NA) giving a total volume of 200 μl. Additional measurements were carried out after including a powerful proteasome inhibitor (MG132, TEBUSA, France), in order to ensure that the activity observed was actually due to the proteasome activity. Kinetic enzymatic activity measurements were carried out at 37°C in a fluorimetric microplate reader (Fluostar Galaxy, BMG, Germany). The excitation and emission wavelengths were 350/440 nm for amino-4-methylcoumarin and 340/410 nm for β-naphthylamine.

Detection of oxidatively modified cytosolic proteins

SDS-PAGE was done using the Laemmli method (Laemmli, 1970) on a 12% acrylamide (w/v) separating gel. Immunoblot detection of carbonyl groups was performed with the OxyBlot oxidized protein detection kit (Abcys Valbiotech, France), according to the manufacturer's instructions. Briefly, 10 μg of proteins were incubated for 15 minutes at room temperature with 2,4-dinitrophenylhydrazine (DNPH) to form the carbonyl derivative dinitrophenylhydrazone before SDS-PAGE separation. After transfer onto nitrocellulose, modified proteins were revealed by anti-DNP antibodies. Detection of bands in immunoblots was carried out (Enhanced ChemiLuminescence, Amersham Biosciences, The Netherlands) using peroxidase-conjugated anti-rabbit secondary antibodies (Amersham Biosciences, Sweden).

Stimulation with TGF-β1 and neutralization of TGF-β1 and TGF-β1 receptor II

Skin HDFs under 55-60% of in vitro proliferative life span were plated at 10,000 cells/cm^2 in BME + 1% FCS. At 72 hours after subcultivation, the cells were stimulated with increasing concentrations of TGF-β1 (R&D systems, UK) diluted in the culture medium for 72 hours.

Neutralization: after the last UVB stress, skin HDFs were incubated with a specific mouse monoclonal antibody against TGF-β1 (3 μg/ml, #mAb240; R&D systems, UK) or with a specific goat polyclonal antibody against the TGF-β1 receptor II (10 μg/ml, #AF-241-NA; R&D systems, UK) as described previously (Tsang et al., 1995; Frippiat et al., 2001). The medium containing the neutralization antibodies was replaced every day for 3 days.

Anti-TGF-β1 and anti-LAP immunofluorescence

Cells were seeded at 1,000 cells/cm^2 in BME +1% FCS on glass cover slides at 16, 40 or 64 hours after the last UVB stress. At 24 hours after seeding, the cells were fixed for 10 minutes with 4% paraformaldehyde (Merck, Germany) in PBS before three washings in PBS and two washings in PBS + 3% BSA (Sigma, USA). The specific goat polyclonal antibody against LAP (TGF-β1) (5 μg/ml, #AF-246-NA; R&D systems, UK) and the specific mouse monoclonal antibody against TGF-β1 (10 μg/ml, #mAb240; R&D systems, UK) were added overnight at 4°C in a wet room. The next day, cells were washed three times in PBS + 3% BSA before the specific Alexa Fluor 488 goat anti-rabbit conjugate (1:1000 dilution, Molecular Probes, USA) and the specific Alexa Fluor 568 goat anti-mouse (1:1000 dilution; Molecular Probes, USA) were added for 1 hour in a wet room at room temperature. Then the protocol for confocal microscopy described above was applied.

Results

A preliminary part of this work was devoted to test whether obvious features of replicative senescence would be observed after a series of 10 exposures of skin HDFs at early cumulative population doublings (CPDs) to UVB (125, 250, 375 or 500 mJ/cm^2) with two stresses per day for 5 days. Cell viability was determined by cell counting, MTT assay (Mosmann, 1983) (data not shown) and protein biomass assay (Lowry, 1951) at 48 hours after the last stress. These methods were previously shown to give comparable results in such models (Dumont et al., 2000). Cytotoxicity was found after exposure to 375 mJ/cm^2 and 500 mJ/cm^2 (Fig. 1A). Therefore the subcytotoxic dose used throughout this study was 250 mJ/cm^2. Using active caspase-3 detection and PARP cleavage as criteria and etoposide as positive pro-apoptotic control, we showed that this UVB intensity was not pro-apoptotic (Fig. 1B,C).

SA β-gal and mitochondrial DNA deletion after repeated exposures to UVB

The UVB-stressed skin HDFs and the senescent skin HDFs were characterized by a major proportion of enlarged cells typical of senescent cultures. The percentage of cells positive for SA β-gal activity increased along the population doublings with 8% of positive cells at early CPDs (day 0) to 53% in cells over 90% of their proliferative life span. A 2.5-fold increase of positive cells was found at 72 hours after 10 exposures to UVB at 250 mJ/cm^2 when compared to the control cells (Fig. 2A).

The so-called common 4,977 bp deletion in the mitochondrial DNA is detected in both replicatively senescent and *t*-BHP-induced senescent HDFs (Dumont et al., 2000). This deletion was detected by nested PCR, performed as explained in the Materials and Methods, after a series of 10 stresses at 250 mJ/cm^2 UVB. Indeed a 404 bp PCR product resulting from the 4,977 bp deletion was observed in UVB-stressed cells at 72 hours after the last stress (Fig. 2Bb). We checked the integrity of the mitochondrial DNA. First we amplified the intact 5,501 bp fragment present in the non-deleted fragment amplified with the H2/L2 primers (data not shown). Second we amplified a conservative 247 bp fragment of the mitochondrial DNA using the primers H1/L1 (Fig. 2Ba).

Decreased proliferative potential after repeated subcytotoxic exposures to UVB

A progressive decrease of the proliferation potential is observed along the population doublings of HDFs (Cristofalo and Sharf, 1973). Determination of the level of incorporation of [^{3}H]thymidine was performed at 24, 48 and 72 hours after a series of 10 UVB stresses at 250 mJ/cm^2. The incorporation remained very low at 48 and 72 hours after the last exposure while it increased sharply in the control cells until they reached confluence at 72 hours after the last stress (Fig. 2C).

Western blottings were performed with proteins extracted at 72 hours after a series of 10 UVB stresses, taking α-tubulin protein level as a reference level. p53, p21^{WAF-1} and p16^{INK-4a} increased by 2.3-, 1.8- and 1.5-fold, respectively when compared to the control cells (Fig. 2D). Active p53 is known to trigger p21^{WAF-1} overexpression. p21^{WAF-1} and p16^{INK-4a} are cyclin-dependent kinase inhibitors that block the cell cycle in G1/S (Sherr and Roberts, 1999). Unpublished results show that the DNA-binding activity of p53 is sharply increased at least until 72 hours after the last UVB stress.

mRNA level of cell cycle- and senescence-associated genes

Apo J, *fibronectin*, *osteonectin* and *SM22* mRNA steady-state levels are increased in senescent HDFs and at 72 hours after exposure of HDFs to *t*-BHP and H_2O_2 (Dumont et al., 2000). We determined these mRNA steady-state levels at 72 hours after a series of 10 exposures to subcytotoxic UVB stress. *p53* and *p21^{WAF-1}* mRNA level was checked since their protein level increased in such conditions.

c-fos and *c-jun* mRNA level were also studied since they are known to be overexpressed in aged skin (Grassilli et al., 1996). Semi-quantitative real-time RT-PCR showed that all these senescence-associated genes tested were overexpressed in both UVB-treated and senescent cells (Fig. 3Aa,b).

We developed a low-density DNA array to check the mRNA level of 240 genes involved in aging or stress (see complete technological description in Materials and Methods). Thirty-nine genes were found to be differentially expressed in UVB-induced SIPS. The list of these genes are listed in Table 2. Most of these genes can be sorted according to their potential involvement in the SIPS phenotype. First, genes involved in growth arrest are overexpressed: *insulin-like growth factor binding protein 3* (*IGF-BP3*) (Buckbinder et al., 1995), *IGF-BP5* (Caroni and Schneider, 1994), *p21^{WAF-1}* (Sherr and Roberts, 1999), *MAX* (Ayer et al., 1993) and proliferating cell nuclear antigen (*PCNA*) (Xu and Morris, 1999). *Cyclin D1* is overexpressed as previously found in replicative senescence (Fukami et al., 1995). Second, a series of proteins involved in chaperoning [*heat shock proteins (Hsp)27, Hsp 40, Hsp 70, Hsp 90, apo J* (Humphreys et al., 1999) or disulfide reduction *metallothionein 2* (*MT2A*) (Jiang et al., 1998)] were overexpressed, as well as *Jun N-terminal kinase-2* (*JNK2*). Antioxidant enzymes like *selenium dependent glutathione peroxidase* (*GPX*) and *peroxiredoxin VI* (Fisher et al., 1999) were also overexpressed. *Metalloproteinases* (*MMP*)*-1* and *MMP-2* were overexpressed. They could participate in the degradation of the extracellular matrix. MMP-1 is known to be overexpressed in in vivo photoaging (Hermann et al., 1993). *Connective tissue growth factor* (*CTGF*) is also overexpressed in UVB-treated cells. It has been shown recently to be upregulated in replicative senescence by a TGF-β-mediated signaling pathway (Kim et al., 2004). It is noteworthy that the type II receptor of TGF-β (*TβRII*) and the pro-inflammatory interleukines *IL-1β* and *IL-11* were also overexpressed. This could participate in the inflammatory aspect of photoaging (Wlaschek et al., 1994). The real-time RT-PCR data and the data obtained with the DualChip human aging were compared for a significant number of differentially expressed genes including: *apo J*, *fibronectin*, *osteonectin*, *SM22*, *p21^{WAF-1}*. Real-time RT-PCR was also used to detect *p53* mRNA, which was found to be increased by 50% (Table 3).

Increased apo J protein level after repeated subcytotoxic exposures to UVB

At 72 hours after a series of 10 exposures to UVB at 250 mJ/cm^2, a 1.5-fold increase of intracellular apo J level was found (with α-tubulin protein level as reference level). More strikingly, a

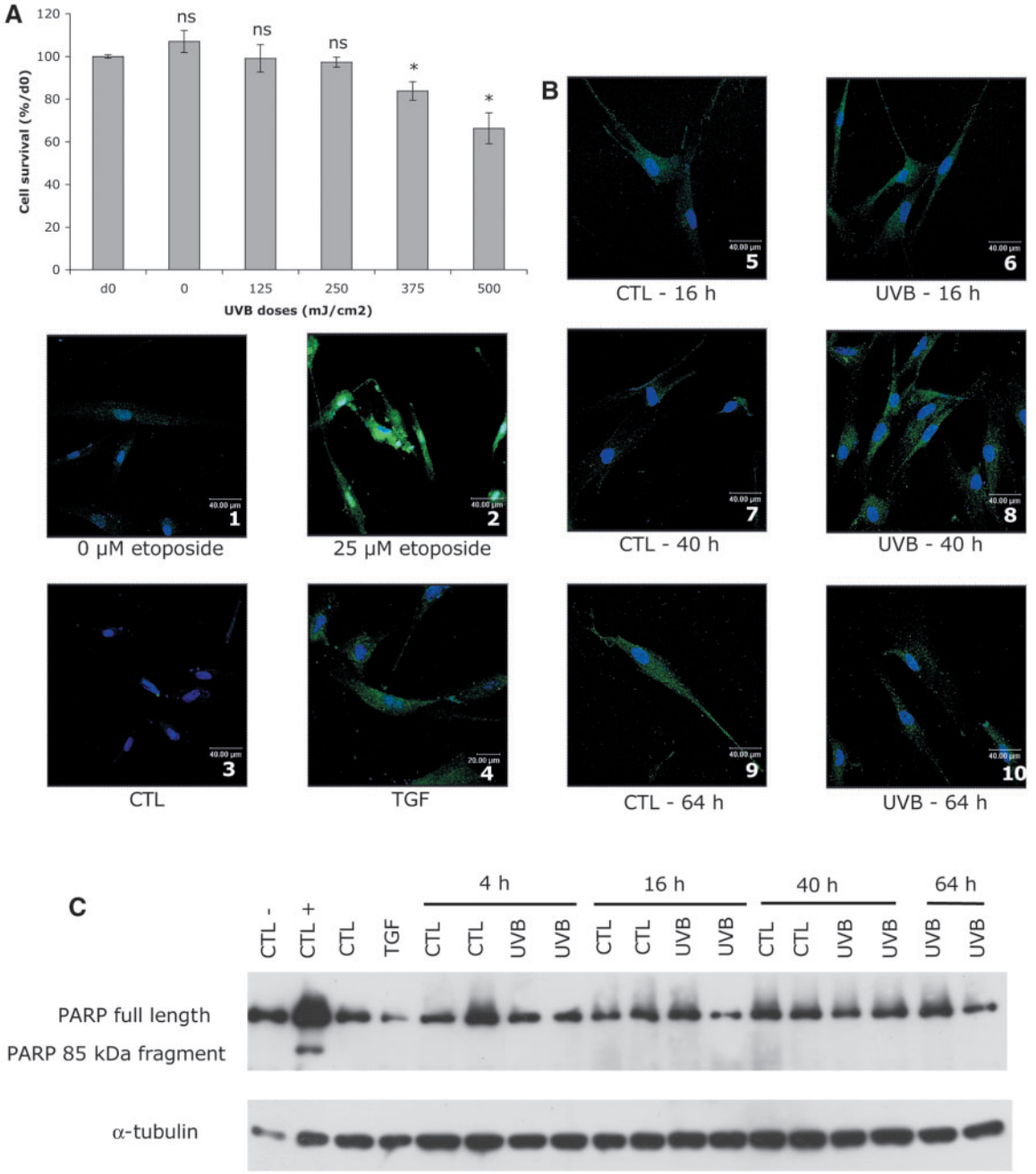

Fig. 1. Exposure to a series of 10 stresses to UVB at 250 mJ/cm2 or 72 hours of stimulation with TGF-β1 do not lead to apoptosis. (A) Cytotoxicity at 24 hours after 10 exposures to UVB. Doses of UVB ranged from 0 to 500 mJ/cm^2 with 2 stresses per day for 5 days. Results are expressed as percentage of cell survival compared to day 0 (d0, 100%) before any stress. Results are given as mean ± s.d. of three independent experiments. Statistical analysis was carried out with Student's *t*-test. ns, non-significant (P>0.05); *, 0.05>P>0.01. (B) No activation of caspase-3 after 10 exposures to UVB at 250 mJ/cm^2 or 72 hours of stimulation with TGF-β1. Semi-quantitative confocal microscopy of skin HDFs that were seeded on glass cover slides at 16, 40 or 64 hours after the last of a series of 10 exposures to UVB at 250 mJ/cm^2 (micrographs 6, 8, 10). Control cells submitted to the same culture conditions but not exposed to UVB were checked (micrographs 5, 7, 9). Cells exposed to etoposide 25 µM for 16 hours were used as positive controls (micrograph 2). Cells incubated for 16 hours in BME were used as negative controls (micrograph 1). At 24 hours after seeding, the activation of caspase-3 was detected using a specific anti-active caspase-3 antibody (green). The nuclei were stained with TO-PRO-3 (blue). No pro-apoptotic effect was found after 72 hours of stimulation with 5 ng/ml of TGF-β1 (micrograph 4) compared with the controls (micrograph 3). (C) No cleavage of PARP after a series of 10 exposures of skin HDFs to UVB at 250 mJ/cm^2 or 72 hours of stimulation with TGF-β1. Skin HDFs were submitted to a series of 10 UVB exposures at 250 mJ/cm^2. Proteins were extracted at 4, 16, 40 or 64 hours after the last stress. Control cells submitted to the same culture conditions but not exposed to UVB were checked. Cells exposed to cytotoxic concentrations of *t*-BHP or not were used as respective positive (CTL +) and negative (CTL –) controls. Total cell extracts were analyzed by western blotting with an anti-PARP-1 antibody. The full length PARP-1 protein (116 kDa) and the fragment resulting for PARP cleavage (85 kDa) are indicated. α-tubulin protein level was used as a reference. No cleavage of PARP was observed after 72 hours of stimulation with 5 ng/ml TGF-β1 (TGF) or not (CTL).

considerable 7.2-fold increase of extracellular apo J was detected in the culture medium collected at 72 hours after the stress series when compared to control counterparts (Fig. 3Ba,b).

Role of apo J against UVB-induced SIPS

Overexpression of both native and tagged form of human apo J in SV-40 WI-38 HDFs favored cell survival when the cells were exposed to cytotoxic doses of UVB and cytotoxic concentrations of ethanol and *t*-BHP. These preliminary results obtained with both forms were similar (data non shown). Apo J cDNA was retrovirally transfected in skin HDFs. Overexpression of both native and tagged form were found at both the mRNA and protein level (Fig. 4Aa,b). Both native and tagged form of apo J protected against the increase of the proportion of SA β-gal-positive cells observed after a series of 10 exposures to 250 mJ/cm^2 UVB (Fig. 4B). Unexpectedly overexpression of both tagged and native apo J decreased the

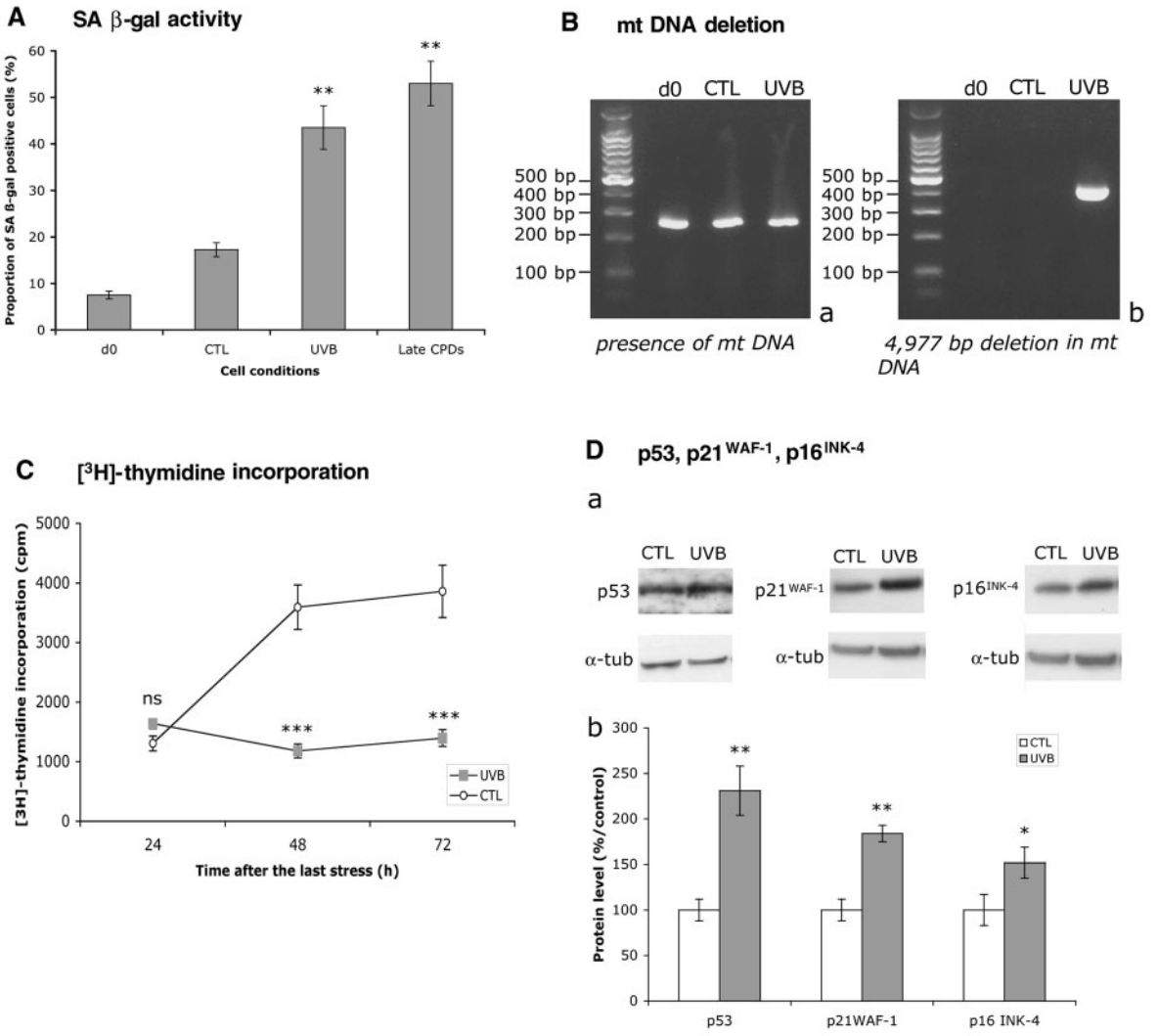

Fig. 2. Effect of a series of 10 exposures of HDFs at early cumulative population doublings (CPDs) to UVB at 250 mJ/cm^2 on SA β-gal activity, common 4,977 bp mitochondrial DNA deletion, incorporation of [^{3}H]thymidine and the protein levels of p53, p21^{WAF-1} and p16^{INK-4A}. (A) Proportion of cells positive for the SA β-gal activity at 72 hours after 10 exposures to UVB at 250 mJ/cm^2. Cells at early CPDs before exposure to UVB (d0), incubated 10 times in a thin layer of PBS without (CTL) or with UVB exposure (UVB) and cells at late CPDs (±90% of their proliferative life span) were examined. Results are given as mean ± s.d. of 3 independent experiments. (B) Detection of the common 4,977 bp mitochondrial DNA deletion by nested PCR after 10 exposures of UVB at 250 mJ/cm^2. (a) Detection of a conserved 247 bp fragment of the mitochondrial DNA in cells incubated 10 times in a thin layer of PBS exposed to UVB (UVB) or not (CTL). Cells at day 0 (d0, before any incubation in PBS) were also examined. (b) Detection of the deletion by nested PCR. The 4,977 bp deletion is detected (404 bp product) in UVB-exposed cells (UVB) and not in CTL or d0 cells. (C) Effect of repeated UVB stresses on the incorporation of [^{3}H]thymidine. Skin HDFs at early CPDs were incubated 10 times in a thin layer of PBS exposed to UVB (250 mJ/cm^2) or not (CTL). They were trypsinised after 24, 48 or 72 hours after the last stress and incubated for 48 hours with [^{3}H]thymidine at 1 μCi. Results are given as mean ± s.d. of three independent experiments. (D) (a) Analysis of p53, p21^{WAF-1} and p16^{INK-4} protein level by western blotting. Proteins were extracted at 72 hours after the last stress. α-tubulin protein was used as reference level. (b) Quantification of the protein level. The results are expressed as 100% of the protein level in control cells (CTL). Results are given as mean ± s.d. of three independent experiments. Statistical analysis was carried out with the Student's *t*-test. ns, non-significant (P>0.05); *, 0.05>P>0.01; **, 0.01>P>0.001; ***, P<0.001.

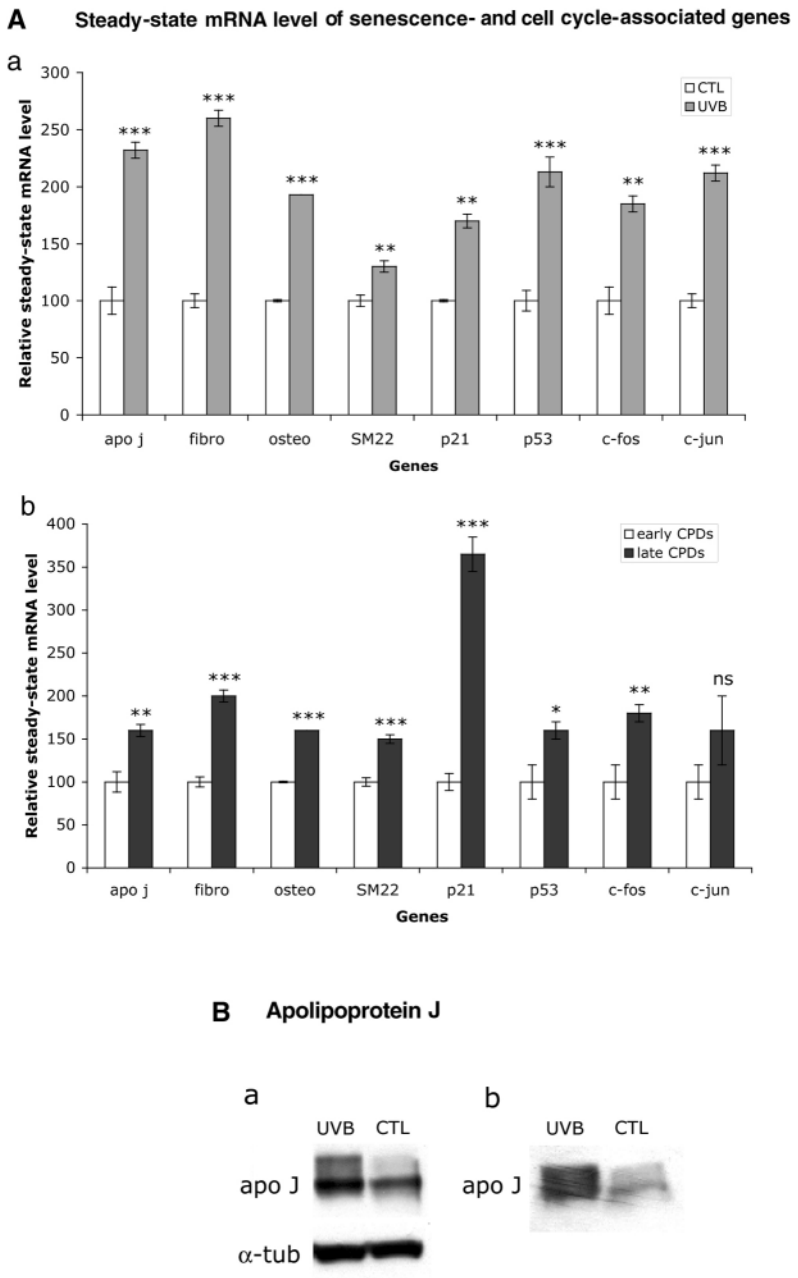

Fig. 3. Effects in HDFs at early cumulative population doublings (CPDs) to 10 exposures of UVB at 250 mJ/cm^2 per exposure on the steady-state mRNA level of senescence- and cell cycle-associated genes, and the level of intracellular and extracellular protein level of apo J. (A) Steady-state mRNA level of *apolipoprotein J* (*apo J*), *fibronectin* (*fibro*), *osteonectin* (*osteo*), *SM22*, *p21^{WAF-1}*, *p53*, *c-fos* and *c-jun*. Total RNA was extracted at 72 hours after the last stress. The GAPDH steady-state mRNA level was used as reference in the real-time RT-PCR. (a) The results obtained from the UVB-treated cells are expressed as percentage of the steady-state mRNA level of the respective mRNA species in control cells (CTL). (b) The results obtained with senescent cells (late CPDs) are compared with cells at early CPDs. Results are given as mean ± s.d. of three independent experiments. (B) Analysis of intracellular (a) and extracellular (b) protein level of apo J by western blotting. Proteins were extracted at 72 hours after the last stress. α-tubulin protein was used as reference level to estimate the intracellular level of apo J while the same volume of collected medium was used to determine the extracellular levels. Statistical analysis was carried out with the Student's *t*-test. ns, non-significant (P>0.05); *, 0.05>P>0.01; **, 0.01>P>0.001; ***, P<0.001.

level of [^{3}H]thymidine incorporation into DNA in both UVB-treated and non-treated cells (Fig. 4C). A possible scenario is metabolic exhaustion due to overexpression of the protein. Previous results obtained with fetal lung WI-38 HDFs suggested that, while being a biomarker of senescence, apo J does not change the proliferative potential of the cells (Petropoulou et al., 2001; Dumont et al., 2002). Moreover, we observed that the growth rate of the skin HDFs used in this study is much lower than that of WI-38 HDFs. This could also explain a differential effect of apo J on proliferation. In the study on *t*-BHP-induced SIPS of WI-38 HDFs, it was shown that overexpression of apo J triggered an overexpression of fibronectin and osteonectin at the mRNA level. Overexpression of osteonectin was shown to inhibit PDGF-induced proliferation but not EGF-, IGF-, FGF- or serum-induced proliferation (Dumont et al., 2002). In the skin HDFs studied here, overexpression of Apo J did not lead to overexpression of fibronectin and osteonectin at the mRNA level (data not shown). Anyway our results suggest no stress-related effect of apo J on [^{3}H]thymidine incorporation. More importantly, the UVB-induced overexpression of fibronectin shown above vanished when apo J was overexpressed (Fig. 4D). Besides apo J, which might play a protective role as extracellular chaperone, we wished to test if the intracellular degradation of modified proteins, through proteasome activity, could be changed in SIPS.

No change of proteasome activity in SIPS induced by acute subcytotoxic stress

An increase in proteasome activity in UVB-induced SIPS might favor a protective effect of proteasome against SIPS whereas a decrease might suggest a pro-SIPS role. It has been proposed that inhibition of proteasome activity could trigger SIPS (Chondrogianni et al., 2003). Exposure of HDFs to hyperoxia under 40% O_2 for several weeks results in SIPS. When the exposure to 40% O_2 is prolonged well after the establishment of SIPS (up to 12 weeks), the proteasome activity sharply decreases (Sitte et al., 2000). In order to test whether proteasome activity also decreases in SIPS induced by acute subcytotoxic stress, we assayed the 20S proteasomal enzymatic activities in four models of SIPS. First SIPS was induced in WI-38 HDFs by a single 2-hour exposure to 300 μM H_2O_2 or five 1-hour exposures to 30 μM *t*-BHP with a daily stress for 5 days (Dierick et al., 2002) and in IMR-90 fetal lung fibroblasts by a single 2-hour exposure to 150 μM H_2O_2 (Frippiat et al., 2001). The results obtained at 72 hours after the last stress were compared with WI-38 HDFs at early and late population doublings. AG04431 skin HDFs in SIPS induced by UVB as

Table 2. Genes differentially expressed in human skin fibroblasts in UVB-induced SIPS

Gene	Name	UVB/CTL	Function	GenBank
IGF-BP3	insulin growth factor binding protein 3	↑ 2,7	growth factor	X64875
HSP70	heat shock 70 kD protein 1	↑ 2,5	defense system	AB023420
HMOX	heme-oxygenase	↑ 2,4	defense system	NM_002133
IL-1B	interleukin 1 beta	↑ 2,4	cytokine	M15330
OSTE	osteonectin	↑ 2,4	extracellular matrix	NM_003118
ODC	ornithine decarboxylase 1	↑ 2,3	cell cycle	NM_002539
HSP90A	heat shock 90 kD protein 1 alpha	↑ 2,3	defense system	X15183
COL1A1	collagen 1 alpha-1	↑ 2,2	extracellular matrix	NM_000088
MAX	MAX protein	↑ 2,2	cell cycle	NM_002382
CTGF	connective tissue growth factor	↑ 2,1	cell cycle	U14750
PCNA	proliferating cell nuclear antigen	↑ 2,1	control of DNA replication	NM002592
TPA	plasminogen activator tissue	↑ 2,1	extracellular matrix	NM_000930
CCND-1	cyclin D1	↑ 2,1	cell cycle	NM_053056
MMP-1	matrix metalloproteinase 1	↑ 2,1	degradation of extracellular matrix	NM_002421
MT2A	metallothionein 2A	↑ 2	defense system	V00594
APO J	apolipoprotein J	↑ 2	defense system	J02908
COL3A1	collagen 3 alpha-1	↑ 2	extracellular matrix	NM_000090
HSP40	heat shock 40 kD protein 1	↑ 2	defense system	D49547
MEK-1	mitogen activated protein kinase kinase 1	↑ 2	cell cycle	L11284
p21	cyclin dependent kinase inhibitor 1A	↑ 1,9	cell cycle	U03106
NRG-1	neuregulin	↑ 1,9	cell cycle	M94165
FN1	fibronectin	↑ 1,9	extracellular matrix	X02761
TGFβRII	transforming growth factor-beta receptor II	↑ 1,9	growth factor	D50685
Il-11	interleukin 11	↑ 1,8	cytokine	NM_000641
MMP-2	matrix metalloproteinase 2	↑ 1,8	degradation of extracellular matrix	NM_004530
ANX-1	annexin 1	↑ 1,8	anti-inflammatory	NM_000700
HSP70B	heat shock 70 kD protein 6	↑ 1,8	defense system	NM_002155
IGF-BP5	insulin growth factor binding protein 5	↑ 1,8	growth factor	M65062
JNK-2	mitogen activated protein kinase 9	↑ 1,8	defense system	U09759
CANX	calnexin	↑ 1,8	cell cycle	NM_001746
HSP27	heat shock 27 kD protein 1	↑ 1,8	defense system	AB020027
EF1A	eucaryotic translation elongation factor-alpha	↑ 1,7	protein synthesis	AY043301
PRX VI	peroxiredoxin VI	↑ 1,7	defense system	NM_004905
MDM2	MDM2	↑ 1,7	cell cycle	NM_002392
GPX	glutathion peroxidase	↑ 1,6	defense system	M21304
H2BS	histone 2B member B/S consensus	↑ 1,6	cell cycle	NM_080593
CCNH	cyclin H	↑ 1,6	cell cycle	NM_001239
FMOD	fibromodulin	↓ 0,6	extracellular matrix	NM_002023
ICAM-1	intracellular adhesion molecule 1	↓ 0,3	extracellular matrix	J031032

Total mRNA was collected at 72 hours after a series of 10 UVB stresses at 250 mJ/cm^2.

described in this work were also included in these assays. We detected a 60% decrease of 20S proteasome activity in replicatively senescent HDFs as already known (Chondrogianni et al., 2003). However, no significant variation could be observed in the four models of SIPS. We tested the hypothesis that proteasome activity did not decrease in SIPS induced by acute subcytotoxic stress because of insufficient stress load. A cytotoxic 2-hour exposure to H_2O_2 was performed and the cellular proteins were extracted at 6 and 72 hours after stress. Significant decreases of 30-45% in 20S proteasomal enzymatic activities were found only at cytotoxic concentrations above 2 mM H_2O_2, at 72 hours after stress (data not shown).

Oxyblot experiments were performed with proteins extracted from respective HDFs exposed to subcytotoxic concentrations of *t*-BHP, UVB and H_2O_2, and from HDFs at early population doublings and in replicative senescence. These oxyblot experiments showed an increase in the amount of oxidized proteins and modifications of the patterns of oxidized proteins in the stressed and the replicatively senescent cells (Fig. 5). These results obtained after assays of proteasome activity and oxyblot experiments suggest that oxidatively damaged proteins are still present in higher amounts when UVB-, *t*-BHP- and H_2O_2-induced SIPS establishes, while proteasome activity is not decreased.

TGF-β1, -β2 and -β3 mRNA level is increased after repeated subcytotoxic exposures to UVB

TGF-β is a multi-functional cytokine involved in cell functions such as cell growth, differentiation and biosynthesis of extracellular connective tissue. TGF-β exists in a number of structurally related isoforms. In mammals, TGF-β1, TGF-β2

Table 3. Comparison between the data obtained with real-time RT-PCR and the DualChip human aging

Gene	Real-time RT-PCR	DNA array	Real time/ array (%)
Apolipoprotein J	2.1	2	4.8
Fibronectin	1.9	1.9	0.0
Osteonectin	1.7	2.4	41.2
SM22	1.2	1.1	8.3
p21	2.1	1.9	9.5
p53	1.5	n.d.	

n.d., not determined.

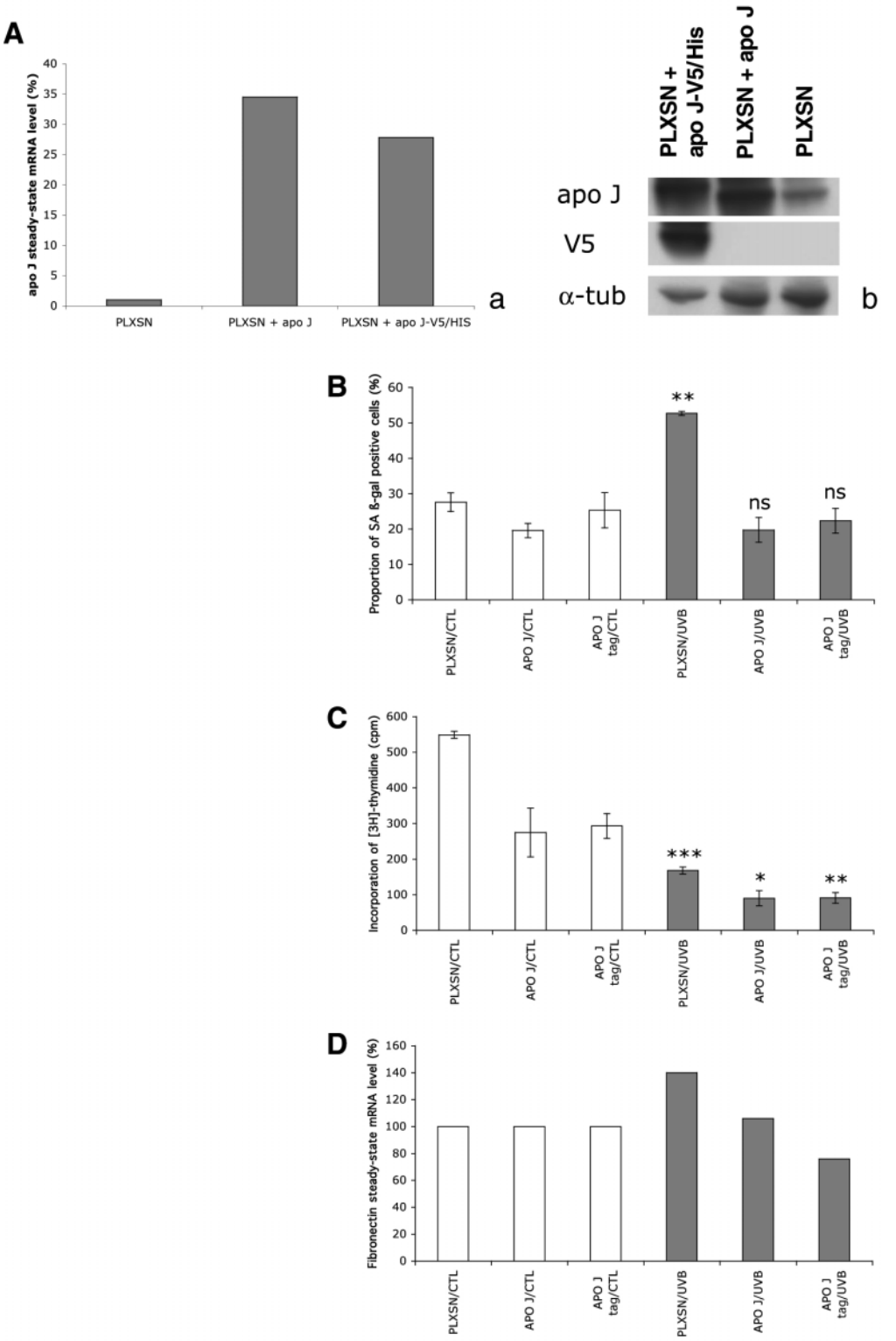

Fig. 4. Effects of retrovirally transfected apo J against UVB-induced SIPS. (A) Overexpression of human apo J after retrovirally-mediated overexpression in skin HDFs. (a) Overexpression at mRNA level of both native and tagged (V5/His) *apo J* compared to empty PLXSN vector. Real time RT-PCR was used to detect *apo J* mRNA. (b) Overexpression of protein level of both native and tagged (V5/His) apo J compared to empty pLXSN vector (western blotting). (B-D) Effects of retrovirally transfected apo J against SIPS induced by 10 subcytotoxic exposures to 250 mJ/cm^2 UVB in skin HDFs. SA β-gal activity (B), incorporation of [^{3}H]thymidine (C) and relative steady-state mRNA level of *fibronectin* (D) were studied as described in Materials and Methods. Skin HDFs transfected with the empty pLXSN vector, with pLXSN/apo J vector or pLXSN/apo J-V5/His vector were exposed (gray columns) or not (white columns) to UVB. Results are given as mean ± s.d. of three independent experiments except (D) where pools of RNA were obtained from extracts of RNA from three independent experiments. Statistical analysis was carried out with the Student's *t*-test. ns, non-significant (P>0.05); *, 0.05>P>0.01; **, 0.01>P>0.001; ***, P<0.001.

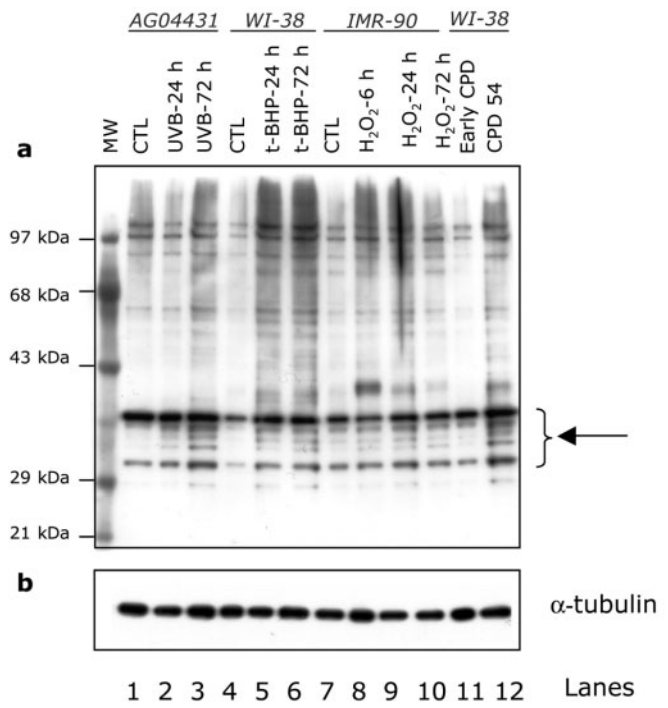

Fig. 5. Oxidized protein patterns in SIPS and replicative senescence. SIPS was induced by 10 exposures of AG04431 HDFs to UVB at 250 mJ/cm^2, five exposures of WI-38 HDFs to *t*-BHP (Dierick et al., 2002), and a single exposure of IMR-90 HDFs to H_2O_2 (Frippiat et al., 2001). Procedures for detecting oxidized proteins are described in Materials and Methods. (a) Lane 1: control AGO4431 HDFs at early cumulative population doublings (CPDs). Lanes 2, 3: AGO4431 HDFs exposed to a series of 10 UVB stresses and proteins extracted at 24 and 72 hours, respectively, after the last stress. Lane 4: control WI-38 cells at early cumulative population doublings. Lanes 5, 6: WI-38 HDFs exposed to a series of 5 *t*-BHP stresses and proteins extracted at 24 and 72 hours, respectively, after the last stress. Lane 7: control IMR-90 cells at early at early cumulative population doublings. Lanes 8, 9, 10: H_2O_2 stressed IMR-90 cells, protein were extracted at 6, 24 and 72 hours, respectively, after the stress. Lanes 11, 12: WI-38 cells at early and late CPDs respectively. MW: molecular weights. (b) α-tubulin was used as reference protein. The arrows indicate the most evident modifications of the oxidized protein patterns.

and TGF-β3 isoforms have been identified (for a review, see Derynck and Zhang, 2003). TGF-β1 has been shown to be involved in H_2O_2-induced SIPS (Frippiat et al., 2001). In vivo, full-thickness, sun-protected adult human skin expressed TGF-β1, -β2 and -β3 transcripts in a ratio of 1:5:3 (Quan et al., 2002). The steady-state mRNA level of TGF-β1, -β2 and -β3 was estimated by semi-quantitative real-time RT-PCR at increasing times after 10 subcytotoxic exposures of skin HDFs to UVB at 250 mJ/cm^2. Glyceraldehyde-3-phosphate dehydrogenase (GAPDH) mRNA level was used as a reference. A respective 2.0-, 1.7- and 1.4-fold overexpression of TGF-β1 was found at 24, 48 and 72 hours after the last UVB stress (Fig. 6A). Such results were similar to those obtained in H_2O_2-induced SIPS of fetal lung HDFs (Frippiat et al., 2001). The steady-state mRNA level of TGF-β2 and -β3 was increased at 72 hours after the last stress by 2.3- and 1.7-fold, respectively (Fig. 6B).

SA β-gal activity and mRNA level of senescence-associated genes increase after stimulation with TGF-β1

Skin HDFs were stimulated for 72 hours with 1, 5 and 10 ng/ml of human TGF-β1 diluted in culture medium + 1% FCS. This range of doses used for the stimulation of skin HDFs with TGF-β1 were not pro-apoptotic. Indeed a stimulation of 5 ng/ml had no effect on the activity of caspase-3 or on PARP cleavage (Fig. 1B,C). The proportion of HDFs positive for SA β-gal activity increased at all TGF-β1 concentrations with a 1.6-fold increase at 5 ng/ml (Fig. 6Ca). However, such increase did not reach the levels obtained after a series of 10 UVB exposures, suggesting partial involvement of TGF-β1.

Semi-quantitative real-time RT-PCR showed that the steady-state mRNA level of the senescence-associated genes *apo J*, *fibronectin*, *osteonectin*, *SM22* and *p21^{WAF-1}* plus *TGF-β1* mRNA was increased after 72 hours of stimulation with 5 ng/ml TGF-β1 (Fig. 6D). When compared to skin HDFs transfected with an empty vector, counterpart cells overexpressing apo J did not display any change in the level of the biomarkers of senescence after stimulation with 5 ng/ml TGF-β1 (data non shown). It is noteworthy that *p53* mRNA level did not change after stimulations with TGF-β1 whereas it increased after a series of 10 exposures to 250 mJ/cm^2 UVB, as shown above. TGF-β1 has already been described as a potential inducer of p21^{WAF-1} (Datto et al., 1995), which is confirmed here at 5 ng/ml TGF-β1 (Fig. 6D).

Increase of both latent and active forms of TGF-β1

TGF-β1 is secreted in a latent form (LTGF-β), which consists of TGF-β1 noncovalently associated with its amino-terminal propeptide called latency associated peptide (LAP) (for a review, see Annes et al., 2003). Extracellular activation of LTGF-β allows the binding of TGF-β to its receptors. Immunohistochemistry has been previously been used with success to discriminate between the latent and active forms of TGF-β1 (Barcellos-Hoff et al., 1995; Chong et al., 1999). Dual immunostaining of LAP (green) and active TGF-β1 (red) after a series of 10 exposures to UVB are shown in Fig. 7. An increase in both latent and active forms of TGF-β1 were detectable at 16, 40 and 64 hours after the last UVB stress in comparison with control cells.

Effects of the neutralization of TGF-β1 and TGF-β1 receptor II

Since our study with the dedicated low-density DNA array showed an increase in the mRNA level of *TGF-β receptor II* (*TβRII*) (Table 2) in UVB-induced SIPS, we wished to test whether neutralization of this receptor with antibodies would block the appearance of UVB-induced SIPS. Neutralizing antibodies against TGF-β1 or TβRII prevented the UVB-induced increase of the proportion of cells positive for SA β-gal activity (Fig. 6Cb). These results corroborate the data obtained by Frippiat et al. (Frippiat et al., 2001) on H_2O_2-induced SIPS. Additionally these authors showed that p38^{MAPK} is activated by TGF-β1 overexpression (Frippiat et al., 2002). When incubated from the ninth exposure to UVB to 72 hours after the last stress with a chemical inhibitor of p38^{MAPK} (SB203580; Calbiochem, USA) skin HDFs failed to display SA β-gal activity and to overexpress *apo J*, *osteonectin* and

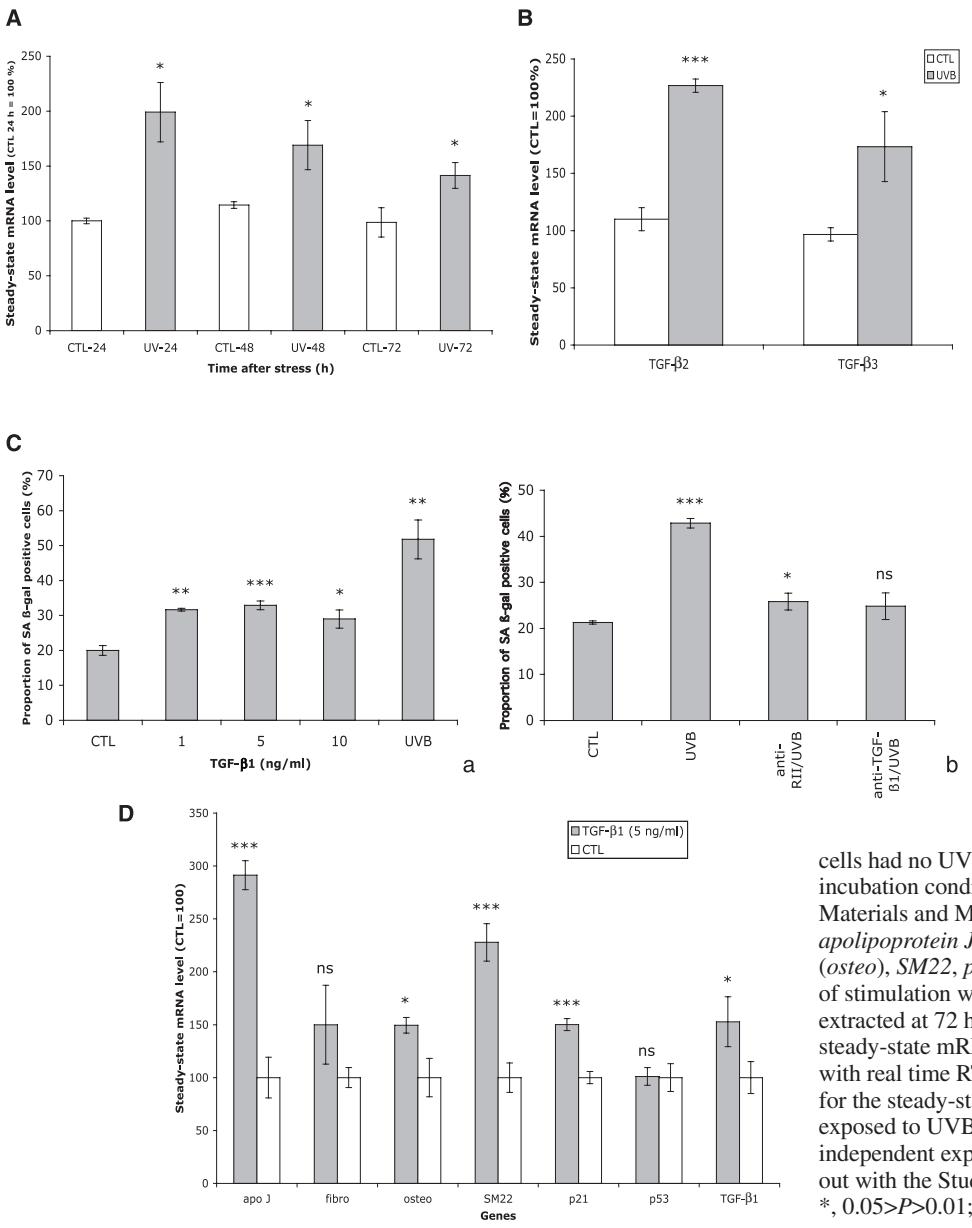

Fig. 6. Role of TGF-β1 in UVB-induced SIPS. (A) Steady-state mRNA level of TGF-β1 in skin HDFs exposed (UVB) or not (CTL) to 10 repeated subcytotoxic doses of UVB at 250 mJ/cm^2. Total RNA samples were extracted at 24, 48 or 72 hours after the last stress. Results were obtained by real-time RT-PCR with *GAPDH* mRNA as reference. The steady-state mRNA level of *TGF-β1* in control cells after 24 hours was considered as 100%. Results are given as mean ± s.d. of three independent experiments. (B) Steady-state mRNA level of TGF-β2 and TGF-β3 at 72 hours after a series of 10 exposures to UVB at 250 mJ/cm2. Results are given as mean ± s.d. of three independent experiments. (Ca) Effects of the stimulation of skin HDFs with TGF-β1 at 1, 5 and 10 ng/ml on the percentage of cells positive for SA β-gal activity after 72 hours of stimulation. Results are given as mean ± s.d. of three independent experiments. (Cb) Effect of anti-TGFβ-1 receptor II and anti-TGF-β1-neutralizing antibodies on the proportion of cells positive for SA β-gal activity at 72 hours after exposure of skin HDFs to 10 subcytotoxic stress with 250 mJ/cm^2 UVB. Control (CTL) cells had no UVB exposure. The concentration and incubation conditions of antibodies are given in the Materials and Methods. (D) Steady-state mRNA level of *apolipoprotein J* (*apo J*), *fibronectin* (*fibro*), *osteonectin* (*osteo*), *SM22*, *p21^{WAF-1}*, *p53* and *TGF-β1* after 72 hours of stimulation with TGF-β1 at 5 ng/ml. Total RNA was extracted at 72 hours after the last stress. The *GAPDH* steady-state mRNA level was considered as reference level with real time RT-PCR. The results are expressed as 100% for the steady-state mRNA level in control cells (CTL) not exposed to UVB. Results are given as mean ± s.d. of three independent experiments. Statistical analysis was carried out with the Student's *t*-test. ns, non-significant (P>0.05); *, 0.05>P>0.01; **, 0.01>P>0.001; ***, P<0.001.

SM22 at the mRNA level (data non shown). In addition, Table 2 shows that MEK-1, a MAPK (mitogen activated protein kinase) kinase able to activate p38^{MAPK} (Wang et al., 2002), is overexpressed at the mRNA level. Preliminary results also suggest that the smad pathway is involved after the UVB-induced SIPS, as an increase in the phosphorylation of smad-2, a receptor-activated smad, was detected at 4, 16 and 40 hours after the last UVB-stress (data non shown).

The antibodies against TGF-β1 also decreased the incorporation of [^{3}H]thymidine into DNA of the cells not exposed to UVB. This suggests that basal levels of TGF-β1 might participate in cell growth as already reported (Kletsas et al., 1995). Similar ratios of [^{3}H]thymidine incorporation existed between the cells exposed to UVB or not and thereafter incubated with the neutralizing antibodies (data non shown). This suggests that TGF-β1 either does not play a major role in the UVB-induced growth arrest or is redundant with other growth arresting mechanisms (for instance p53) as observed in H_2O_2-induced SIPS (Frippiat et al., 2001). Real-time RT-PCR was used to determine the steady-state mRNA levels of *fibronectin*, *osteonectin*, *SM22*, *apo J*, *p21^{WAF-1}* and *TGF-β1* after 72 hours incubation with neutralizing antibodies against TGF-β1 following a series of 10 subcytotoxic exposures to UVB. Although a stress-induced overexpression of each gene was observed, these overexpressions vanished when the cells were incubated with the neutralizing antibodies (Fig. 8). In these experiments pools of total RNA were obtained from three independent experiments.

Discussion

Skin represents an excellent and accessible model organ allowing the study of intrinsic and extrinsic factors coordinately contributing to the complex phenomenon of aging (for a review, see Wlaschek et al., 2001). Evidence shows that intrinsic and extrinsic aging of the skin are probably driven by

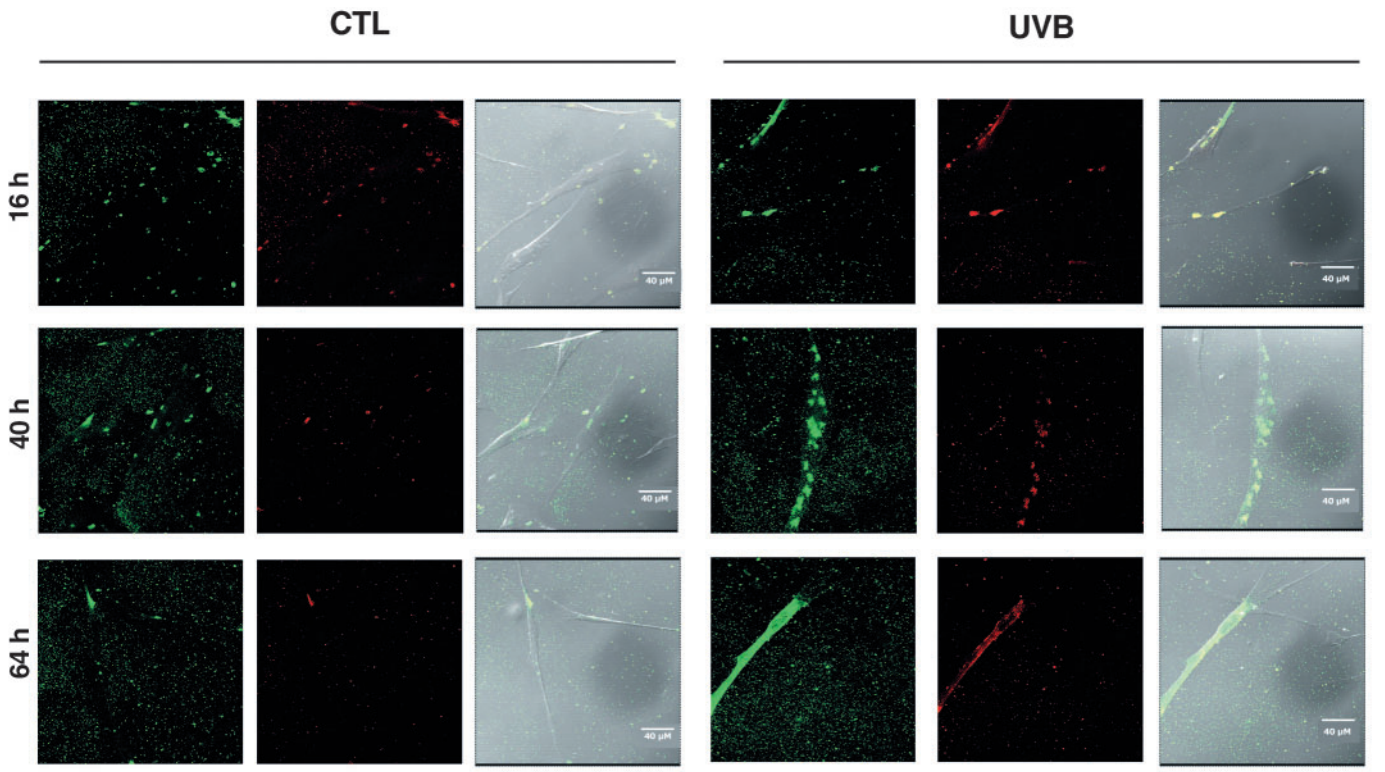

Fig. 7. A series of 10 exposures of skin HDFs to UVB at 250 mJ/cm^2 increases sharply the abundance of both latent and active forms of TGF-β1. Skin HDFs were given a series of 10 exposures to UVB at 250 mJ/cm^2 and seeded on glass cover slides at 16, 40 or 64 h after the last stress. Control cells were submitted to the same culture conditions but not exposed to UVB. At 24 hours after seeding, the activation of TGF-β1 was investigated by immunofluorescence using antibodies recognizing the latent form of TGF-β1 (LAP) (green; left images) and the active TGF-β1 (red; middle images) using semi-quantitative confocal microscopy. (Right images) Superimposition of phase contrast and fluorescence with green and red emission.

similar biological, biochemical and molecular mechanisms (for a review, see Rittie and Fisher, 2002). Extrinsic aging, also called photoaging, is mainly due to UV-induced damage of the dermal connective tissue of the skin, resulting in qualitative and quantitative alterations of the dermal extracellular matrix (for a review, see Wlaschek et al., 2003). Dermal fibroblasts are essential regulators of the synthesis and the degradation of extracellular matrix. UVB generates DNA damage, particularly cyclobutane pyrimidine dimers and (6-4) photoproducts (for a review, see Ichihashi et al., 2003) and severe oxidative stress in skin via interactions with intracellular chromatophores and photosensitizers. This results both in transient and permanent genotoxicity, and in the activation of cytoplasmic signal transduction pathways related to growth, differentiation, replicative senescence and connective tissue degradation (for a review, see Rittie and Fisher, 2002). Very few of the multiple studies that dealt with the effects of UV were aimed at investigating the long-term effects of UV.

In this study we developed a model of premature senescence induced by a series of 10 exposures to a subcytotoxic dose of UVB (250 mJ/cm^2). Repeated exposures to UVB sharply increased SA β-gal activity, reaching levels observed after exposure(s) of fetal lung HDFs to *t*-BHP or H_2O_2 (Dumont et al., 2000). Higher levels of SA β-gal-positive cells were previously found in keratinocytes and fibroblasts from skin biopsies from old donors compared with younger counterparts (Dimri et al., 1995). Nested PCR was necessary to detect the DNA fragment resulting from the 4,977 bp deletion, indicating an extremely low frequency of this deletion, as also suggested by studies on senescent HDFs and on HDFs in *t*-BHP-induced SIPS (Dumont et al., 2000). It was reported that the in vivo frequency of this deletion was higher in sun-exposed compared with non-exposed skin biopsies taken from the same individuals (Pang et al., 1994). This deletion was confined to the dermal rather than the epidermal compartment of the skin and seems to reflect photo- rather than chronological aging (Birch-Machin et al., 1998). This deletion has been shown to be mediated by singlet oxygen (Berneburg et al., 1999).

Growth arrest is an important feature of cellular senescence. A drastically decreased proliferative potential of HDFs in UVB-induced SIPS was observed after 10 exposures to UVB. This decreased potential was correlated with an overexpression of p53, $p21^{WAF-1}$ and $p16^{INK-4A}$. The overexpression of p53 protein and DNA binding activity would play a role in growth arrest, while the overexpression of TGF-β would play a role in the appearance of the other biomarkers of senescence after a series of 10 exposures to UVB. The results on p53 and $p21^{WAF-1}$ corroborate more fragmentary results obtained with skin BJ fibroblasts ectopically expressing telomerase (BJ1-hTERT) or not, and exposed to a single H_2O_2 stress and five UVB stresses (de Magalhaes et al., 2002). However, BJ1-hTERT cells undergo tremendous changes in gene expression when compared with normal cells (de Magalhaes et al., 2004), BJ and BJ1-hTERT cells are much more resistant to oxidative

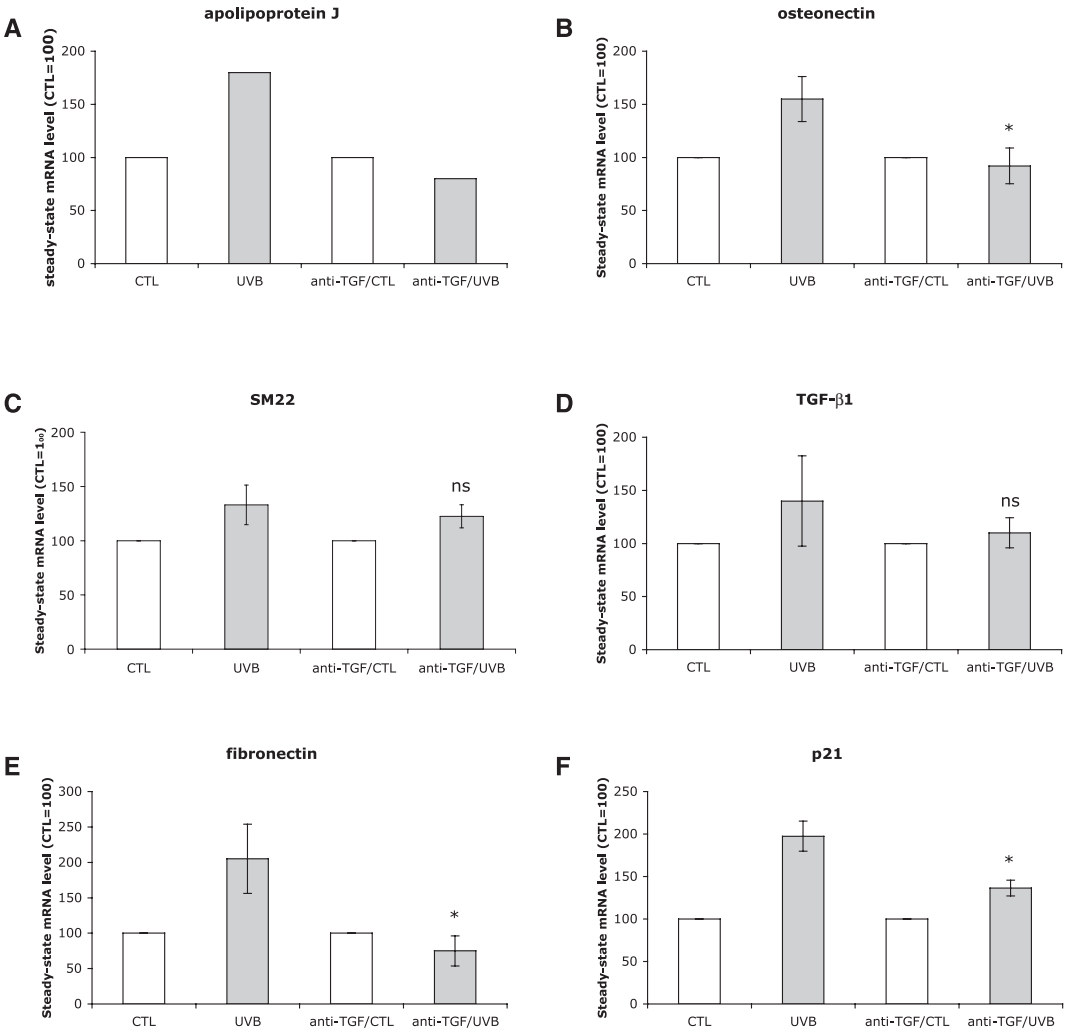

Fig. 8. Effects of anti-TGF-β1 neutralizing antibody (3 μg/ml) on the steady-state mRNA level of apolipoprotein J (A), *osteonectin* (B), *SM22* (C), *TGF-β1* (D), *fibronectin* (E) and $p21^{WAF-1}$ (F) at 72 hours after a series of 10 exposures of skin HDFs to UVB at 250 mJ/cm^2. Anti-TGF-β1 CTL and CTL cells had no UVB exposure and were incubated with or without anti-TGF-β1 antibodies, respectively. Statistical analysis was carried out with the Student's *t*-test. ns, non-significant (P>0.05); *, 0.05>P>0.01.

stress than most fibroblasts strains (Lorenz et al., 2001) and do not overexpress $p16^{INK-4A}$ or TGF-β1 after UVB stress, whereas TGF-β1 overexpression is observed in vivo after exposure to UVB, reinforcing the present model in which skin HDFs are exposed to a series of 10 stresses.

The relative steady-state mRNA level of *c-jun*, *c-fos*, *MMP-1* and *MMP-2* increased in dermal HDFs at 72 hours after a series of 10 UVB exposures. It was already known that *c-jun* is overexpressed at the mRNA and protein levels in vivo after exposure of human skin to UV (Fisher et al., 1998). Increased levels of c-JUN protein compete with JunD resulting in the preferential formation of c-JUN:c-FOS AP-1 complexes in both the epidermis and the dermis (Angel et al., 2001). AP-1 regulates the expression of several metalloproteinases (MMP-1, MMP-3 and MMP-9), whose overexpression has been correlated with the activation of AP-1 by UV irradiation (Wlaschek et al., 2003).

The senescence-related genes *fibronectin*, *osteonectin*, *SM22* and *apo J* were overexpressed at 72 hours after the last UVB stress. Fibronectin is an essential component of the extracellular matrix and may contribute to the morphological changes observed in senescent HDFs as well as anchorage of cells to their substrate (Kumazaki et al., 1993). Osteonectin is a calcium-binding protein able to inhibit the cell entry into S phase through selective binding of platelet-derived growth factor (Funk and Sage, 1991). SM22 (transgelin) encodes a putative calcium binding protein involved in senescence-induced morphological changes (Lecka-Czernick et al., 1996). Apo J is an extracellular protein with chaperone-like activity similar to small heat shock proteins (Poon et al., 2002; Humphreys et al., 1999). The steady-state mRNA levels of these four genes increased in replicative senescence and in H_2O_2- and *t*-BHP-induced SIPS (Dumont et al., 2000), which broadens their role in cellular senescence.

WI-38 HDFs retrovirally transfected with gp80, the canine apo J sharing 88% homology with its human counterpart, better resisted exposures to cytotoxic concentrations of *t*-BHP or ethanol and better resisted *t*-BHP- and ethanol-induced SIPS

(Dumont et al., 2002). As observed here transfection of human apo J in SV-40 WI-38 cells favors survival after cytotoxic exposures to UVB, *t*-BHP and ethanol. Additionally, dermal HDFs retrovirally transfected with human apo J were protected against the increase of both SA β-gal-positive cells and fibronectin mRNA steady-state mRNA level induced by UVB. It is noteworthy that apo J expression has been reported to be regulated by TGF-β1 via modulation of c-fos (Jin and Howe, 1999). This suggest that cells in SIPS could be better protected against further stresses of similar intensities.

The results obtained when assaying proteasome activity and performing oxyblots left open a possibility for a role of damaged proteins somehow activating signaling pathways that could eventually participate in the establishment of SIPS, in agreement with the findings of Chondrogianni et al. (Chondrogianni et al., 2003).

Exposure of fetal lung IMR-90 HDFs to a subcytotoxic concentration of H_2O_2 induces a first phase of activation of $p38^{MAPK}$ (Frippiat et al., 2002). This activation triggers an overexpression of TGF-β1, which starts a positive feedback loop allowing sustained activation of $p38^{MAPK}$. $p38^{MAPK}$ phosphorylates and activates the transcription factor ATF-2 that interacts with hypophosphorylated retinoblastoma protein (pRb). This complex induces the appearance of features of replicative senescence. This regulatory loop triggers UVB-induced SIPS with concomitant activation of p53. Indeed TGF-β1 is known to be overexpressed in skin in vivo after UVB exposure (Quan et al., 2002). In addition, UVB is known to generate ROS (for a review, see Ichihashi et al., 2003), and ROS have been shown to activate the latent form of TGF-β1 (Vodovotz et al., 1999). Thus there might be two successive waves of activation of TGF-β1 after subcytotoxic exposures to UVB: an immediate activation by ROS, followed by an increase of the secretion of the latent form of TGF-β1, possibly activated by MMP-2, as shown earlier (Yu and Stamenkovic, 2000).

The specific biological functions of each TGF-β isoforms and their role in photoaging and tumorigenesis in human skin remain to be elucidated. In addition investigating the signaling pathway(s) leading to UVB-induced SIPS could be informative about the role of TGF-β1 in skin photoaging.

F. Debacq-Chainiaux is a Research Assistant and O. Toussaint is a Research Associate of the FNRS, Belgium. V. Royer and G. Carrard were post-doctoral fellows of the european project 'Protage' (contract no. QLK6-CT-1999-02193). We also thank the european projects 'Functionage' (contract no. QLK6-2001-00310), 'Geha' (contract no. LSHM-CT-2004-503270) and 'CRAFT-Cellage' (contract no. CRAFT-1999-71628) as well as the Region Wallonne projects 'Modelage' and 'TOXISIPS', and the Region Wallonne/FSE project 'Arrayage' (EPH 3310300 R0472/215316). We thank Dr C. Michiels for providing extracts of *t*-BHP-treated cells.

References

Angel, P., Szabowski, A. and Schorpp-Kistner, M. (2001). Function and regulation of AP-1 subunits in skin physiology and pathology. *Oncogene* **20**, 2413-2423.

Annes, J. P., Munger, J. S. and Rifkin, D. B. (2003). Making sense of latent TGFbeta activation. *J. Cell Sci.* **116**, 217-224.

Ayer, D. E., Kretzner, L. and Eisenman, R. N. (1993). Mad: a heterodimeric partner for Max that antagonizes Myc transcriptional activity. *Cell* **72**, 211-222.

Barcellos-Hoff, M. H., Ehrhart, E. J., Kalia, M., Jirtle, R., Flanders, K. and Tsang, M. L. (1995). Immunohistochemical detection of active transforming growth factor-beta in situ using engineered tissue. *Am. J. Pathol.* **147**, 1228-1237.

Bayreuther, K., Rodemann, H. P., Hommel, R., Dittmann, K., Albiez, M. and Francz, P. I. (1988). Human skin fibroblasts *in vitro* differentiate along a terminal cell lineage. *Proc. Natl. Acad. Sci. USA* **85**, 5112-5116.

Berneburg, M., Grether-Beck, S., Kurten, V., Ruzicka, T., Briviba, K., Sies, H. and Krutmann, J. (1999). Singlet oxygen mediates the UVA-induced generation of the photoaging-associated mitochondrial common deletion. *J. Biol. Chem.* **274**, 15345-15349.

Birch-Machin, M. A., Tindall, M., Turner, R., Haldane, F. and Rees, J. L. (1998). Mitochondrial DNA deletions in human skin reflect photo- rather than chronologic aging. *J. Invest. Dermatol.* **110**, 149-152.

Brack, C., Lithgow, G., Osiewacz, H. and Toussaint, O. (2000). Molecular and cellular gerontology. *EMBO J.* **19**, 1929-1934.

Buckbinder, L., Talbott, R., Velasco-Miguel, S., Takenaka, I., Faha, B., Seizinger, B. R. and Kley, N. (1995). Induction of the growth inhibitor IGF-binding protein 3 by p53. *Nature* **377**, 646-649.

Bulteau, A. L., Petropoulos, I. and Friguet, B. (2000). Age-related alterations of proteasome structure and function in aging epidermis. *Exp. Gerontol.* **35**, 767-777.

Caroni, P. and Schneider, C. (1994). Signaling by insulin-like growth factors in paralyzed skeletal muscle: rapid induction of IGF1 expression in muscle fibers and prevention of interstitial cell proliferation by IGF-BP5 and IGF-BP4. *J. Neurosci.* **14**, 3378-3388.

Chainiaux, F., Magalhaes, J. P., Eliaers, F., Remacle, J. and Toussaint, O. (2002). UVB-induced premature senescence of human diploid skin fibroblasts. *Int. J. Biochem. Cell Biol.* **34**, 1331-1339.

Chen, Q. M., Bartholomew, J. C., Campisi, J., Acosta, M., Reagan, J. D. and Ames, B. N. (1998). Molecular analysis of H_2O_2-induced senescent-like growth arrest in normal human fibroblasts: p53 and Rb control G1 arrest but not cell replication. *Biochem. J.* **332**, 43-50.

Chondrogianni, N., Stratford, F. L., Trougakos, I. P., Friguet, B., Rivett, A. J. and Gonos, E. S. (2003). Central role of the proteasome in senescence and survival of human fibroblasts: induction of a senescence-like phenotype upon its inhibition and resistance to stress upon its activation. *J. Biol. Chem.* **278**, 28026-28037.

Chong, H., Vodovotz, Y., Cox, G. W. and Barcellos-Hoff, M. H. (1999). Immunocytochemical localization of latent transforming growth factor-beta1 activation by stimulated macrophages. *J. Cell Physiol.* **178**, 275-283.

Cristofalo, V. J. and Sharf, B. B. (1973). Cellular senescence and DNA synthesis. Thymidine incorporation as a measure of population age in human diploid cells. *Exp. Cell Res.* **76**, 419-427.

Datto, M. B., Li, Y., Panus, J. F., Howe, D. J., Xiong, Y. and Wang, X. F. (1995). Transforming growth factor beta induces the cyclin-dependent kinase inhibitor p21 through a p53-independent mechanism. *Proc. Natl. Acad. Sci. USA* **92**, 5545-5549.

de Longueville, F., Surry, D., Meneses-Lorente, G., Bertholet, V., Talbot, V., Evrard, S., Chandelier, N., Pike, A., Worboys, P., Rasson, J. P. et al. (2002). Gene expression profiling of drug metabolism and toxicology markers using a low-density DNA microarray. *Biochem. Pharmacol.* **64**, 137-149.

de Magalhaes, J. P., Chainiaux, F., Remacle, J. and Toussaint, O. (2002). Stress-induced premature senescence in BJ and hTERT-BJ1 human foreskin fibroblasts. *FEBS Lett.* **523**, 157-162.

de Magalhaes, J. P., Chainiaux, F., de Longueville, F., Mainfroid, V., Migeot, V., Marcq, L., Remacle, J., Salmon, M. and Toussaint, O. (2004). Gene expression and regulation in H_2O_2-induced premature senescence of human foreskin fibroblasts expressing or not telomerase. *Exp. Gerontol.* **39**, 1379-1389.

Derynck, R. and Zhang, Y. E. (2003). Smad-dependent and Smad-independent pathways in TGF-beta family signalling. *Nature* **425**, 577-584.

Dierick, J. F., Kalume, D. E., Wenders, F., Salmon, M., Dieu, M., Raes, M., Roepstorff, P. and Toussaint, O. (2002). Identification of 30 protein species involved in replicative senescence and stress-induced premature senescence. *FEBS Lett.* **531**, 499-504.

Dimri, G. P., Lee, X., Basile, G., Acosta, M., Scott, G., Roskelley, C., Medrano, E. E., Linskens, M., Rubelj, I., Pereira-Smith, O. et al. (1995). A biomarker that identifies senescent human cells in culture and in aging skin *in vivo*. *Proc. Natl. Acad. Sci. USA* **92**, 9363-9367.

Dumont, P., Burton, M., Chen, Q. M., Gonos, E. S., Frippiat, C., Mazarati, J. B., Eliaers, F., Remacle, J. and Toussaint, O. (2000). Induction of replicative senescence biomarkers by sublethal oxidative stresses in normal human fibroblast. *Free Radic. Biol. Med.* **28**, 361-373.

Dumont, P., Chainiaux, F., Eliaers, F., Petropoulou, C., Remacle, J., Koch-Brandt, C., Gonos, E. S. and Toussaint, O. (2002). Overexpression of apolipoprotein J in human fibroblasts protects against cytotoxicity and premature senescence induced by ethanol and tert-butylhydroperoxide. *Cell Stress Chaperones* **7**, 23-35.

Filser, N., Margue, C. and Richter, C. (1997). Quantification of wild-type mitochondrial DNA and its 4,8-kb deletion in rat organs. *Biochem. Biophys. Res. Comm.* **233**, 102-107.

Fisher, A. B., Dodia, C., Manevich, Y., Chen, J. W. and Feinstein, S. I. (1999). Phospholipid hydroperoxides are substrates for non-selenium glutathione peroxidase. *J. Biol. Chem.* **274**, 21326-21334.

Fisher, G. J., Talwar, H. S., Lin, J., Lin, P., McPhillips, F., Wang, Z., Li, X., Wan, Y., Kang, S. and Voorhees, J. J. (1998). Retinoic acid inhibits induction of c-Jun protein by ultraviolet radiation that occurs subsequent to activation of mitogen-activated protein kinase pathways in human skin in vivo. *J. Clin. Invest.* **101**, 1432-1440.

Frippiat, C., Chen, Q. M., Zdanov, S., Magalhaes, J. P., Remacle, J. and Toussaint, O. (2001). Subcytotoxic H_2O_2 stress triggers a release of transforming growth factor-beta 1, which induces biomarkers of cellular senescence of human diploid fibroblasts. *J. Biol. Chem.* **276**, 2531-2537.

Frippiat, C., Dewelle, J., Remacle, J. and Toussaint, O. (2002). Signal transduction in H_2O_2-induced senescence-like phenotype in human diploid fibroblasts. *Free Radic. Biol. Med.* **33**, 1334-1346.

Fukami, J., Anno, K., Ueda, K., Takahashi, T. and Ide, T. (1995). Enhanced expression of cyclin D1 in senescent human fibroblasts. *Mech. Ageing Dev.* **81**, 139-157.

Funk, S. E. and Sage, E. H. (1991). The Ca2(+)-binding glycoprotein SPARC modulates cell cycle progression in bovine aortic endothelial cells. *Proc. Natl. Acad. Sci. USA* **88**, 2648-2652.

Grassilli, E., Bellesia, E., Salomoni, P., Croce, M. A., Sikora, E., Radziszewska, E., Tesco, G., Vergelli, M., Latorraca, S., Barbieri, D. et al. (1996). c-fos/c-jun expression and AP-1 activation in skin fibroblasts from centenarians. *Biochem. Biophys. Res. Commun.* **226**, 517-523.

Helenius, M., Makelainen, L. and Salminen, A. (1999). Attenuation of NF-kappaB signaling response to UVB light during cellular senescence. *Exp. Cell Res.* **248**, 194-202.

Herrmann, G., Wlaschek, M., Lange, T. S., Prenzel, K., Goerz, G. and Scharffetter-Kochanek, K. (1993). UVA irradiation stimulates the synthesis of various matrix-metalloproteinases (MMPs) in cultured human fibroblasts. *Exp. Dermatol.* **2**, 92-97.

Humphreys, D. T., Carver, J. A., Easterbrook-Smith, S. B. and Wilson, M. R. (1999). Clusterin has chaperone-like activity similar to that of small heat shock proteins. *J. Biol. Chem.* **274**, 6875-6881.

Ichihashi, M., Ueda, M., Budiyanto, A., Bito, T., Oka, M., Fukunaga, M., Tsuru, K. and Horikawa, T. (2003). UV-induced skin damage. *Toxicology* **189**, 21-39.

Jiang, L. J., Maret, W. and Vallee, B. L. (1998). The ATP-metallothionein complex. *Proc. Natl. Acad. Sci. USA* **95**, 9146-9149.

Jin, G. and Howe, P. H. (1999). Transforming growth factor beta regulates clusterin gene expression via modulation of transcription factor c-Fos. *Eur. J. Biochem.* **263**, 534-542.

Kim, K. H., Park, G. T., Lim, Y. B., Rue, S. W., Jung, J. C., Sonn, J. K., Bae, Y. S., Park, J. W. and Lee, Y. S. (2004). Expression of connective tissue growth factor, a biomarker in senescence of human diploid fibroblasts, is up-regulated by a transforming growth factor-beta-mediated signaling pathway. *Biochem. Biophys. Res. Commun.* **318**, 819-825.

Kletsas, D., Stathakos, D., Sorrentino, V. and Philipson, L. (1995). The growth-inhibitory block of TGF-β is located close to the G1/S border in the cell cycle. *Exp. Cell Res.* **217**, 477-483.

Kumazaki, T., Kobayashi, M. and Mitsui, Y. (1993). Enhanced expression of fibronectin during in vivo cellular aging of human vascular endothelial cells and skin fibroblasts. *Exp. Cell Res.* **205**, 396-402.

Laemmli, U. K. (1970). Cleavage of structural proteins during the assembly of the head of bacteriophage T4. *Nature* **227**, 680-685.

Lecka-Czernik, B., Moerman, E., Jones, R. A. and Goldstein, S. (1996). Identification of genes sequences overexpressed in senescent and Werner sydrome human fibroblasts. *Exp. Gerontol.* **31**, 159-174.

Lorenz, M., Saretzki, G., Sitte, N., Metzkow, S. and von Zglinicki, T. (2001). BJ fibroblasts display high antioxidant capacity and slow telomere shortening independent of hTERT transfection. *Free Radic. Biol. Med.* **31**, 824-831.

Lowry, O., Rosebrought, N., Farr, A. and Randall, R. (1951). Protein measurement with Folin phenol reagent. *J. Biol. Chem.* **193**, 265-275.

Mosmann, T. (1983). Rapid colorimetric assay for cellular growth and survival: application to proliferation and cytotoxicity assays. *J. Immunol. Methods* **65**, 55-63.

Pang, C. Y., Lee, H. C., Yang, J. H. and Wei, Y. H. (1994). Human skin mitochondrial DNA deletions associated with light exposure. *Arch. Biochem. Biophys.* **312**, 534-538.

Petropoulou, C., Trougakos, I. P., Kolettas, E., Toussaint, O. and Gonos, E. S. (2001). Clusterin/apolipoprotein J is a novel biomarker of cellular senescence that does not affect the proliferative capacity of human diploid fibroblasts. *FEBS Lett.* **509**, 287-297.

Poon, S., Treweek, T. M., Wilson, M. R., Easterbrook-Smith, S. B. and Carver, J. A. (2002). Clusterin is an extracellular chaperone that specifically interacts with slowly aggregating proteins on their off-folding pathway. *FEBS Lett.* **513**, 259-266.

Quan, T., He, T., Kang, S., Voorhees, J. J. and Fisher, G. J. (2002). Ultraviolet irradiation alters transforming growth factor beta/smad pathway in human skin in vivo. *J. Invest. Dermatol.* **119**, 499-506.

Rittie, L. and Fisher, G. J. (2002). UV-light-induced signal cascades and skin aging. *Ageing Res. Rev.* **1**, 705-720.

Rosette, C. and Karin, M. (1996). Ultraviolet light and osmotic stress: activation of the JNK cascade through multiple growth factor and cytokine receptors. *Science* **274**, 1194-1197.

Shay, J. W. and Wright, W. E. (2000). Hayflick, his limit and cellular aging. *Nat. Rev. Mol. Cell. Biol.* **1**, 72-76.

Sherr, C. J. and Roberts, J. M. (1999). CDK inhibitors: positive and negative regulators of G1-phase progression. *Genes Dev.* **13**, 1501-1512.

Sitte, N., Merker, K., von Zglinicki, T., Grune, T. and Davies, K. J. (2000). Protein oxidation and degradation during cellular senescence of human BJ fibroblasts: part I – effects of proliferative senescence. *FASEB J.* **14**, 2495-2502.

Tsang, M. L., Zhou, L., Zheng, B. L., Wenker, J., Fransen, G., Humphrey, J., Smith, J. M., O'Connor-McCourt, M., Lucas, R. and Weatherbee, J. A. (1995). Characterization of recombinant soluble human transforming growth factor-beta receptor type II (rhTGF-beta sRII). *Cytokine* **7**, 389-397.

Vodovotz, Y., Chesler, L., Chong, H., Kim, S. J., Simpson, J. T., DeGraff, W., Cox, G. W., Roberts, A. B., Wink, D. A. and Barcellos-Hoff, M. H. (1999). Regulation of transforming growth factor beta 1 by nitric oxide. *Cancer Res.* **59**, 2142-2149.

Wang, W., Chen, J. X., Liao, R., Deng, Q., Zhou, J. J., Huang, S. and Sun, P. (2002). Sequential activation of the MEK-extracellular signal-regulated kinase and MKK3/6-p38 mitogen-activated protein kinase pathways mediates oncogenic ras-induced premature senescence. *Mol. Cell. Biol.* **22**, 3389-3403.

Wlaschek, M., Heinen, G., Poswig, A., Schwarz, A., Krieg, T. and Scharffetter-Kochanek, K. (1994). UVA-induced autocrine stimulation of fibroblast-derived collagenase/MMP-1 by interrelated loops of interleukin-1 and interleukin-6. *Photochem. Photobiol.* **59**, 550-556.

Wlaschek, M., Tantcheva-Poor, I., Naderi, L., Ma, W., Schneider, L. A., Razi-Wolf, Z., Schuller, J. and Scharffetter-Kochanek, K. (2001). Solar UV irradiation and dermal photoaging. *J. Photochem. Photobiol. B* **63**, 41-51.

Wlaschek, M., Ma, W., Jansen-Durr, P. and Scharffetter-Kochanek, K. (2003). Photoaging as a consequence of natural and therapeutic ultraviolet irradiation – studies on PUVA-induced senescence-like growth arrest of human dermal fibroblasts. *Exp. Gerontol.* **38**, 1265-1270.

Xu, J. and Morris, G. F. (1999). p53-mediated regulation of proliferating cell nuclear antigen expression in cells exposed to ionizing radiation. *Mol. Cell. Biol.* **19**, 12-20.

Yu, Q. and Stamenkovic, I. (2000). Cell surface-localized matrix metalloproteinase-9 proteolytically activates TGF-beta and promotes tumor invasion and angiogenesis. *Genes Dev.* **14**, 163-176.

Zhivotovsky, B. and Kroemer, G. (2004). Apoptosis and genomic instability. *Nat. Rev. Mol. Cell Biol.* **5**, 752-762.

Table S1

Suplementary data Table 1

Gene	Name	Function
23kd	23KDa Highly basic protein	protein synthes
ACTB	Beta-Actin	morphology
ADAM1	A disintegrin and metalloproteinase domain1	extracellular m
ADPRT	polysynthetase	DNA repair
Aldo	Aldolase A,	glycolysis
ANX1	Annexin1	differentiation
APOB	ApoliproteinB	
APOE	ApoliproteinE	extracellular m
APOJ	ApoliproteinJ	defense system
AREG	Amphiregulin	
ATM	Ataxia telangiectasia mutated	cell cycle/DNA
BAT1	Nuclear-RNA-helicase	DNA repair
BAX	BCL2-associated X protein	apoptosis (+)
BCL2	B-cell lymphoma2	apoptosis (-)
BCLX	BCLX	apoptosis (-)
BMP2	Bone morphogenetic protein2	apoptosis
BRCA2	Breast cancer2	cell cycle/DNA
CANX	calnexin	cell cycle/DNA
CASP7	caspase7	apoptosis (+)
CASP8	Caspase8	apoptosis (+)
CCNA1	cyclinA1	cell cycle/DNA
CCNB1	cyclinB1	cell cycle/DNA
CCND1	cyclinD1	cell cycle/DNA
CCND2	cyclinD2	cell cycle/DNA
CCND3	cyclinD3	cell cycle/DNA
CCNE1	CyclinE	cell cycle/DNA
CCNF	CyclinF	cell cycle/DNA
CCNG	CyclinG	apoptosis
CCNH	cyclinH	cell cycle/DNA
CDC42	Cell division cycle42	morphology
CDK2	Cyclin dependent kinase2	cell cycle/DNA
CDK4	Cyclin dependent kinase4	cell cycle/DNA
CENPA	centromere-protein-A	chromosomal c
CENPF	mitosin	chromosomal c
C-FOS	c-fos	cell cycle/DNA
CKB	creatin-kinase-brain	metabolism
COL15A1	collagenXV-alpha1	extracellular m
COL1A1	Collagen1-alpha1	extracellular m
COL3A1	collagenIII-alpha1	extracellular m
COL6A2	collagenVI-alpha2	extracellular m
COX1	Prostaglandin endoperoxidase synthase1	inflammation

COX2	Prostaglandin endoperoxidase synthase2	inflammation
CROC1A	Ubiquitin conjugating enzyme E2 variant1	cell cycle/DNA
CST6	cystatin-M	extracellular m
CTGF	Connective tissue growth factor	cell cycle/DNA
CTSD	cathepsinD	extracellular m
CTSH	cathepsinH	extracellular m
CTSS	cathepsinS	extracellular m
CTSZ	cathepsinZ	extracellular m
cyc	Cyclophilin 33A	protein synthes
CYT2A	Keratin2	differentiation
DHFR	Dihydrofolate reductase	cell cycle/DNA
DPT	dermatopontin	extracellular m
DSG1	desmoglein1	differentiation
E2F1	E2F transcription factor1	cell cycle/DNA
E2F5	E2F transcription factor5	cell cycle/DNA
EAR1	Nuclear receptor subfamily1, group D, member 1	cell cycle/DNA
EF1A	Eukaryotic translation elongation factor-alpha1	chromosomal c
EGR1	Early growth response1	defense system
EGR2	Early growth response2	cell cycle/DNA
EGR3	Early growth response3	defense system
EIF-4A	Eukaryotic translation initiation factor 4A	
ELN	elastin	extracellular m
EPC1	Enhancer of polycomb1	cell cycle/DNA
ETFB	electron-transfert-flavoprotein-beta	metabolism
EWSR1	Ewing sarcoma breakpoint region1	cell cycle/DNA
FE65	Fe65	apoptosis
FES	Feline sarcoma oncogene	cell cycle/DNA
FLG	filaggrin	differentiation
FMOD	fibromodulin	extracellular m
FN1	fibronectin	extracellular m
G6PD	glucose-6-phosphate-dehydrogenase	metabolism
GAA	glucosidase-II-precursor	metabolism
GADD153	DNA damage inducible transcript3	DNA repair
GAPD	Glyceraldehyde-3-phosphate-dehydrogenase	glycolysis
GLB1	Beta1-galactosidase	differentiation
GMCSF	Colony stimulating factor2	
GPX	glutathione peroxidase	defense system
GRB2	Growth factor receptor-bound protein2	defense system
GSTP1	Glutathione S-transferase pi	
GSTT1	Glutathione S-transferase theta1	
H2B/S	histone2b member B/S consensus	cell cycle/DNA
H3FF	histone3 member F consensus	cell cycle/DNA
H4FM	histone4 member M consensus	cell cycle/DNA
HBEGF	Heparin binding epidermal growth factor transcript	
HLF	Hepatic leukemia factor	defense system
HMOX	heme-oxygenase	defense system
HSP27	Heat shock 27kD protein1	defense system
HSP40	Heat shock 40kD protein1	defense system
HSP70	Heat shock 70kD protein1	defense system

HSP70B	Heat shock 70kD protein6	defense system
HSP90-alpha	Heat shock 90kD protein1 alpha	defense system
ICAM-1	Intracellular adhesion molecule1	extracellular m
ID1	Inhibitor of DNA binding1	cell cycle/DNA
ID2	Inhibitor of DNA binding2	cell cycle/DNA
IFNG	Interferon gamma	cytokine
IGF1	Insulin like growth factor1	growth factor
IGF1R	Insulin like growth factor1 receptor	growth factor
IGFBP2	Insulin growth factor binding protein2	growth factor
IGFBP3	Insulin growth factor binding protein3	growth factor
IGFBP5	Insulin growth factor binding protein5	growth factor
IL10	Interleukin 10	cytokine
IL11	Interleukin 11	cytokine
IL11RA	Interleukin 11-receptor-alpha	cytokine
IL12	Interleukin 12	cytokine
IL15	Interleukin 15	cytokine
IL1A	Interleukin1 alpha	cytokine
IL1B	Interleukin1 beta	cytokine
IL2	Interleukin 2	cytokine
IL3	Interleukin 3	cytokine
IL4	Interleukin 4	cytokine
IL6	Interleukin 6	cytokine
IL8	Interleukin 8	cytokine
INT6	Translation initiation factor3 subunit6	morphology
IVL	involucrin	differentiation
JNK1	Mitogen activated protein kinase8	defense system
JNK2	Mitogen activated protein kinase9	defense system
JNKK1	Mitogen activated protein kinase kinase 4	defense system
JUND	Jun D proto-oncogene	defense system
Ki-67	Ki-67	
KNSL5	mitotic-kinesin-like-protein1	chromosomal c
KNSL6	mitotic-centromere-associated-kinesin	chromosomal c
KRT1	keratin1	differentiation
HK1	Hexokinase 1	glycolysis
KRT10	keratin10	differentiation
KRT14	keratin14	differentiation
KRT16	keratin16	differentiation
KRT17	keratin17	differentiation
HPRT	Hypoxanthine phosphoribosyltransferase 1	HouseKeeping
KRT19	Keratin19	differentiation
KRT6A	Keratin6	differentiation
L6	Transmembrane4 superfamily member1	
MAP17	Membrane associated protein17	
MAX	MAX protein	cell cycle/DNA
MCM2	Mitotin	DNA replicatior
MDM2	MDM2	cell cycle/DNA
MEK1	Mitogen activated protein kinase kinase1	cell cycle/DNA
MEK2	Mitogen activated protein kinase kinase2	cell cycle/DNA
MMP1	matrix metalloproteinase 1	extracellular m

		(degradation)
MMP10	matrix metalloproteinase 10	extracellular m
		(degradation)
MMP11	matrix metalloproteinase 11	extracellular m
		(degradation)
MMP12	matrix metalloproteinase 12	extracellular m
		(degradation)
MMP13	matrix metalloproteinase 13	extracellular m
		(degradation)
MMP14	matrix metalloproteinase 14	extracellular m
		(degradation)
MMP15	matrix metalloproteinase 15	extracellular m
		(degradation)
MMP2	matrix metalloproteinase 2	extracellular m
		(degradation)
MMP3	matrix metalloproteinase 3	extracellular m
		(degradation)
MMP7	matrix metalloproteinase 7	extracellular m
		(degradation)
MDH	Malate dehydrogenase 1	HouseKeeping
MP1	Metalloprotease1	extracellular m
		(degradation)
MSRA	methionine-sulfoxide-reductase A/peptide	protein repair
MT2A	metallothionein 2A	defense system
MVK	mevalonate-kinase	
MYBL2	b-myb	cell cycle/DNA
MYC	c-myc	cell cycle/DNA
NCK1	NCK adaptor protein1	cell cycle/DNA
NF1	neurofibromin1	cell cycle/DNA
NGFR	nerve growth factor receptor	defense system
NRG1	neuregulin	
ODC	Ornithine decarboxylase1	cell cycle/DNA
OPG	osteoprotegerin	extracellular m
OPN	osteopontin	migration
Oste	osteonectin	extracellular m
p16	Cyclin dependent kinase inhibitor 2A	cell cycle
p21	Cyclin dependent kinase inhibitor 1A	cell cycle
p27	Cyclin dependent kinase inhibitor 1B	cell cycle
p35	Cyclin dependent kinase5 regulatory subunit1	cell cycle
p53	Tumor protein p53	cell cycle
p57	Cyclin dependent kinase inhibitor 1C	cell cycle
PAI1	plasminogen activator inhibitor type1	extracellular m
PAI2	plasminogen activator inhibitor type2/Urokinase inhibitor	extracellular m
PAK	P21 activated kinase1	morphology
PCNA	Proliferating cell nuclear antigen	cell cycle/DNA
PKM2	pyruvate-kinase-muscle	metabolism
PLAU	urokinase	
PLAUR	urokinase-receptor	
PLK	Polo-like kinase	cell cycle/DNA
PLA2	Phospholipase A2	HouseKeeping
POLA2	Polymerase alpha	cell cycle/DNA
PRSS11	Protease serine11	
PRX VI	Peroxiredoxin VI	defense system

PSMA2	proteasome (prosome, macropain) subunit, alpha type, 2	protein degrad
PSMA3	proteasome (prosome, macropain) subunit, alpha type, 3	protein degrad
PSMC6	proteasome (prosome, macropain) 26S subunit, non-ATPase, 6	protein degrad
PSMD1	proteasome (prosome, macropain) 26S subunit, non-ATPase, 1	protein degrad
PSMD11	proteasome (prosome, macropain) 26S subunit, non-ATPase, 11	protein degrad
PSMD12	proteasome (prosome, macropain) 26S subunit, non-ATPase, 12	protein degrad
PSOR1	psoriasin	
RAF1	c-raf-1	cell cycle/DNA
RANTES	Small inducible cytokine A5	
RB1	Retinoblastome1	cell cycle
RET	ret protooncogene	cell cycle/DNA
ROR1	R AR related orphan receptorA	cell cycle/DNA
RPL3	60S-ribosomal-proteinL3	
RPS10	ribosomal-protein S10	
RRAS	R-ras	cell cycle/DNA
RRM1	ribonucleotide-reductase M1	cell cycle/DNA
S9	Ribosomal Proteine S9	protein synthes
S100A10	Calpactin1	differentiation
S100A11	Calgizzarin	differentiation
S100A8	calprotectin	inflammation
SHC	SHC transforming protein1	apoptosis
SLK	Ste-20-related serine/threonine kinase	apoptosis
SLP2	Stomatin like protein2	cell cycle/DNA
SM22	transgelin	muscle develop
SMAD1	Mother against decapentalplegic homol1	morphology
SNCG	synuclein	cell cycle/DNA
SDS	Serine Dehydratase	HouseKeeping
SOD2	Superoxide dismutase2	defense system
SPRR1B	cornifin	differentiation
SRI	sorcin	defense system
STAT5	Signal transducer and activator of transcription 5A	cell cycle/DNA
TBXA2R	Thromboxane-A2-receptor	cell cycle/DNA
TERC	telomerase-RNA	cell cycle/DNA
TERT	telomerase-reverse transcriptase	cell cycle/DNA
TFAP2A	Transcription factor AP2-alpha	cell cycle/DNA
TFAP2B	Transcription factor AP2-beta	cell cycle/DNA
TFAP2C	Transcription factor AP2-gamma	cell cycle/DNA
TGFA	TGF-alpha	growth factor
TGFB1	TGF-beta1	growth factor
TGFBR2	TGF-beta-R2	growth factor
TGM1	transglutaminase1	differentiation
TH	Tyrosine-hydroxylase	
THBS1	Thrombospondin	extracellular m
TIMP1	Tissue inhibitor of metalloproteinase1	extracellular m
TIMP2	Tissue inhibitor of metalloproteinase2	extracellular m
TK1	thymidine-kinase	cell cycle/DNA
TNFA	tumor necrosis factor alpha	cytokine

TFR	Transferrin receptor	HouseKeeping
TNFB	tumor necrosis factor beta	cytokine
TNFRSF1A	TNF-alpha-RI	cytokine
TNFRSF1B	TNF-alpha-RII	cytokine
TOP2A	topoisomerase2-alpha	cell cycle/DNA
TPA	Plasminogen activator tissue	extracellular m
TRF1	Telomeric repeat binding factor1	cell cycle/DNA
Tubu	Alpha-tubulin	morphology
TYMS	thymidylate-synthetase	cell cycle/DNA
UBE2C	Ubiquitin conjugating enzyme E2C/ubiquitin carrier protein	protein degrad
VEGFC	Vascular endothelial growth factor C	cell cycle/DNA
VEGFR1	Vascular endothelial growth factor receptor1	cell cycle/DNA